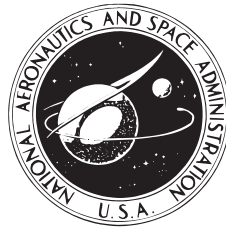


NASA TECHNICAL NOTE



NASA TN D-6125

NASA TN D-6125

**INVESTIGATION AND CALCULATIONS
OF BASIC PARAMETERS FOR
THE APPLICATION OF THE LASER
DOPPLER VELOCIMETER**

*by James F. Meyers
Langley Research Center
Hampton, Va. 23365*

NATIONAL AERONAUTICS AND SPACE ADMINISTRATION . WASHINGTON, D. C. . APRIL 1971

1. Report No. NASA TN D-6125	2. Government Accession No.	3. Recipient's Catalog No.	
4. Title and Subtitle INVESTIGATION AND CALCULATIONS OF BASIC PARAMETERS FOR THE APPLICATION OF THE LASER DOPPLER VELOCIMETER		5. Report Date April 1971	
		6. Performing Organization Code	
7. Author(s) James F. Meyers		8. Performing Organization Report No. L-7441	
		10. Work Unit No. 125-24-04-19	
9. Performing Organization Name and Address NASA Langley Research Center Hampton, Va. 23365		11. Contract or Grant No.	
		13. Type of Report and Period Covered Technical Note	
12. Sponsoring Agency Name and Address National Aeronautics and Space Administration Washington, D.C. 20546		14. Sponsoring Agency Code	
		15. Supplementary Notes	
16. Abstract The paper presents a method of determining the operating criteria necessary to operate a laser Doppler velocimeter. The basic theory used to determine the criteria is presented and programed in a computer program. The results of the program are obtained for the cross-beam technique in its three modes of operation. From the basic theory and the program, a test case was chosen to determine the best laser Doppler velocimeter to use for the test flow and the parameters required for proper operation.			
17. Key Words (Suggested by Author(s)) Laser Laser applications Turbulent measurement techniques Laser Doppler velocimeter		18. Distribution Statement Unclassified - Unlimited	
19. Security Classif. (of this report) Unclassified	20. Security Classif. (of this page) Unclassified	21. No. of Pages 65	22. Price * \$3.00

Contents

	Page
Summary	1
Introduction	2
Symbols	3
Comparison Between the Single-Beam and Cross-Beam Systems	7
System Theory	9
Derivation of the Relation between Signal-to-Noise Ratio and Scattered Laser Power	9
Rayleigh and Mie Scattering Functions	13
Expansion of Basic Theory	14
Application of Basic Theory	17
Development of a Computer Program	17
Results of Application of the Program	17
Determination of Operating Criteria for an LDV in a Test Flow	22
Errors	24
Concluding Remarks	25
Appendix A - Derivation of Doppler Frequency	27
Appendix B - Determination of the Effects of Rayleigh Scatter	32
Appendix C - Computer Program for Calculation of LDV Parameters	34
References	51
Figures	52

INVESTIGATION AND CALCULATIONS OF BASIC PARAMETERS FOR THE APPLICATION OF THE LASER DOPPLER VELOCIMETER

James F. Meyers
Langley Research Center

Summary

This paper is concerned with a recent development in a nonprobe technique for velocity measurement, namely, the laser Doppler velocimeter (LDV). The technique makes use of the Doppler effect on scattered laser radiation from small particles in the gas flow. Two LDV techniques currently in use, those being the single-beam technique and the cross-beam technique, are described and compared. The three modes of operation of the cross-beam technique are compared with respect to the output characteristics and particle density requirements in the flow. The dual-scatter-forward-scatter mode is shown to be the most efficient. The dual-scatter-back-scatter mode, although not as efficient, has advantages which make the mode desirable for some applications.

A computer program involving the basic LDV theory is presented and is used to derive the results for the comparison of the three modes in the cross-beam system. These results included the output signal-to-noise ratio and required seeding density as a function of the input laser power and scattering angle. By using a modified version of the program, the required input laser power was determined as a function of molecular density for a fixed signal-to-noise ratio, based on only molecular scatter.

A test example is presented to show how the basic theory and the computer program are used to determine the operating criteria required for LDV operation in a particular flow in a wind tunnel at Mach 6.

Introduction

The aerodynamist and gas dynamist are very interested in turbulent gas flows and, in particular, in determining various turbulent-flow parameters such as the velocity vector components.

In the past few years a nonprobe technique has been under development by several research groups (as reported in refs. 1, 2, 3, and 4) that will measure the instantaneous velocity at a point in the flow. The technique involves scattering laser light from gas molecules and small particles in the flow. Due to the Doppler effect on the scattered light, the velocity vector components can be determined and the flow can be characterized. This system is generally called the laser Doppler velocimeter (LDV).

Since the advent of the laser, much work has been done on the study of scattered laser light from gas molecules and small particles suspended in the gas. This work has been mainly concerned with atmospheric study using the Light Detection and Ranging technique (ref. 5). Work has also been performed on the development of theory used to describe the operation of the LDV. The purpose of this study is to investigate broadly the relation between the scattering of light from moving particles and the apparatus necessary to extract velocity information from the scattered light. Presently, the LDV characteristics are calculated independent of one another and related experimentally. This method can do little to predict the parameter requirements for LDV operation in a particular flow. By relating all LDV characteristics, LDV systems may be theoretically applied to any flow under consideration. A computer program presented in this paper contains the related theory necessary to calculate all LDV parameters. The resulting plots of a study presented in the paper relate signal-to-noise ratio, photomultiplier output current and power, required seeding density, and spatial resolution with the LDV scattering angle. The scattering angle and the photodetector frequency response determine the upper limit of particle velocity that can be measured. Thus, all LDV characteristics are related and considered.

The program has been applied to two LDV configurations currently in use. These are the single-beam system in the reference-scatter mode and the cross-beam system in the reference-scatter, dual-scatter-forward-scatter, and dual-scatter-back-scatter modes. As an example of the use of the program in determining the required parameters for LDV operation, a typical gas flow is analyzed for possible application of an LDV to survey the velocity field.

Symbols

The symbols in brackets are the equivalent symbols used in the computer program.

A_{CL}	[ACL]	cross-sectional area of receiver optics, meters ²
A_r	[AR]	area of receiving lens, meters ²
B	[B]	statistical factor due to dynode emission
c	[C]	velocity of light, 3×10^8 meters/second
D	[D]	diameter of input aperture, meters
D_a	[DA]	Airy disk diameter at sample volume, meters
D_r	[DR]	diameter of receiving lens, meters
$E_r \cos \omega_r t$		reference electromagnetic wave, volts/meter
$E_s \cos \omega_s t$		scattered electromagnetic wave, volts/meter
E_t		total electromagnetic wave, $E_r \cos \omega_r t + E_s \cos \omega_s t$, volts/meter
e	[E]	electron charge, 1.6×10^{-19} coulomb
F	[F]	laser power density at sampling point, watts/meter ²
F_l	[F1]	input lens focal length, meters
f		depolarization attributable to an isotropy of scatterer
f_D		light frequency observed by stationary observer of laser beam scattering from moving particle, Hertz
f_L		laser frequency, Hertz
f_o		light frequency observed by stationary observer positioned along velocity vector of moving light source, Hertz

f_p		light frequency observed by moving particle from stationary laser source, Hertz
f_s		source light frequency, Hertz
g_p	[G]	gain of photomultiplier
h	[H]	Plancks constant, 6.626×10^{-34} joule-second
$i(t)$	[XIOUT]	total photomultiplier output current, amperes
$i_{dc}(t)$		dc component of photomultiplier output current, amperes
$i_{if}(t)$		ac component of photomultiplier output current, amperes
$i(\alpha_1, n, \theta)$	[XIMIE]	Mie intensity function, $\frac{i_{\perp}(\alpha_1, n, \theta) + i_{\parallel}(\alpha_1, n, \theta)}{2}$
$i_{\perp, \parallel}(\alpha_1, n, \theta)$		intensity of light with electric vector perpendicular and parallel to plane through direction of propagation of incident and scattered beams, respectively
$\langle i_{if}^2 \rangle$		mean-square photodetector response, amperes ²
$\langle i_n^2 \rangle$		mean-square noise response in detector due to shot noise, amperes ²
k	[XK]	wave number of incident radiation, $2\pi/\lambda$, meter ⁻¹
L	[XL]	length of sample volume, meters
N	[XN]	number of photons per second impinging on photocathode surface, photons/second
N_{Mie}	[XNMIE]	number density of particles at sample volume, particles/meter ³
N_r		number density of molecules at sample volume, molecules/meter ³
n	[SREF]	index of refraction
P	[PO]	input laser power, watts

P_r		unscattered laser power used as reference signal, watts
P_o	[XPOUT]	output power of photomultiplier, dBm
P_s	[PS]	scattered laser power used as signal, watts
P_{sc}	[PSC]	laser power scattered from flow in acceptance cone of receiver, watts
q		attenuation of wave (transmissivity) in propagating from scatterer to detector lens
R	[R]	output impedance of matching unity gain amplifier on photomultiplier, ohms
r		radius of particle, meters
s_l	[SLAST]	final particle diameter, microns
s_s	[S]	starting particle diameter, microns
S/N		signal-to-noise ratio
$(S/N)_{dB}$	[SN]	signal-to-noise ratio, decibels
t		time, seconds
V_s		particle velocity, meters/second
Z	[Z]	distance from receiving lens to sample volume, meters
α		angle between particle velocity vector and laser beam, degrees
α_1	[S]	particle size parameter, $2\pi r/\lambda$
$\bar{\alpha}$		average polarizability of air, meters ³
β		proportionality constant of photomultiplier
Δ		depolarization factor
ΔS	[DELTA]	incremental particle diameter, microns

ΔV	[V]	sample volume in flow, meters ³
$\Delta\theta$	[DETH]	incremental cross-beam angle, degrees
Δf	[DELF]	noise bandwidth, hertz
Δf_D		Doppler frequency, hertz
ε		transmission coefficient of receiver optics
ε_1	[EL1]	transmission coefficient of receiving lens
ε_2	[EL2]	transmission coefficient of beam splitter
η	[XNU]	quantum efficiency of photomultiplier
θ		angle between unscattered laser beam and signal optics, degrees
θ_1	[DTHELA]	final cross-beam angle, degrees
θ_s	[DTHETA]	starting cross-beam angle, degrees
θ'		angle between laser beam and scattered beam, degrees
λ	[XLAM]	wavelength of laser beam, meters
ν		optical frequency of laser, hertz
σ_{Mie}		Mie scattering cross section per unit volume, meter ⁻¹
σ_r		Rayleigh scattering cross section per unit volume, meter ⁻¹
Φ		angle of rotation of receiver optics about sample volume in cross-beam system, degrees
ϕ_1		angle between velocity vector and beam 1 in cross-beam system, degrees
ϕ_2		angle between crossed laser beams, degrees
Ω		solid angle viewed by signal optics, steradians

ω_r	angular frequency of reference electromagnetic wave, radians/second
ω_s	angular frequency of signal electromagnetic wave, radians/second

Comparison Between the Single - Beam and Cross-Beam Systems

The laser Doppler velocimeter as developed by Foreman, George, and Lewis (ref. 1) has been used to measure accurately high-velocity flows in wind tunnels without disturbing the flow as with previous techniques (ref. 2). This system, which will be referred to as the reference-scatter single-beam system, employs a focused laser beam which is scattered from particles in the gas flow. A portion of the scattered light is sampled and mixed with a portion of the unscattered laser beam and collected by an optical-photomultiplier system where the two light beams heterodyne to yield the difference frequency between the two light beams. This difference frequency, or Doppler frequency, is related to the particle velocity in the flow. Particles of micron size are expected to follow the gas velocity within a few percent and, for the purposes of this study, are assumed to do so. The relationship between the particle velocity and Doppler frequency, as developed in appendix A as equation (A10), is

$$\Delta f_D = \frac{V_s}{\lambda} (\cos(\alpha - \theta') - \cos \alpha)$$

where	Δf_D	Doppler frequency, Hz
	V_s	particle velocity, m/s
	λ	wavelength of laser beam, m
	α	angle between particle velocity vector and laser beam, deg
	θ'	angle between laser beam and scattered light, deg

A typical reference-scatter single-beam LDV is shown in figure 1.

A new LDV technique has recently been developed (ref. 3) which involves an optical system that divides the input laser beam into two parallel beams which are then focused to a point, thus crossing the two

beams. If a particle is located at the crossover point, the particle will scatter light from both beams. By placing a photomultiplier along the axis of one of the beams, a reference-scatter system is constructed, since the photomultiplier also collects scattered radiation from the other beam. Since the scattered radiation from the other beam radiates in all directions, part of this scattered light is coaxial and parallel with the reference beam and thus automatically aligns the photomultiplier. This technique is referred to as the cross-beam system and is shown in figure 2.

If the receiving optics for the cross-beam system were located at a position midway between the two beams, the optics would then collect scattered light from both laser beams. Since the scattered light collected from each beam is of a different frequency, a heterodyne frequency is obtained. This configuration is shown in figure 3. From the theoretical development in appendix A, it is shown that the heterodyne frequency which is equal to the Doppler frequency is independent of the placement of the receiver optics, as long as the receiver optics are in the plane of the beams. The Doppler frequency thus derived (eq. (A18)) is

$$\Delta f_D = \frac{2V_s}{\lambda} \sin \frac{\phi_2}{2}$$

where	Δf_D	Doppler frequency, Hz
	V_s	particle velocity, m/s
	λ	laser wavelength, m
	ϕ_2	angle between two laser beams, deg

It can now be seen that the dual-scatter technique has an advantage over the reference-scatter technique. By referring to equation (A10), it is found that the Doppler frequency is dependent upon the angle of viewing the scattered radiation θ' . Thus the Doppler frequency will vary across the viewing lens since the finite lens views a band of scattering angles. This problem is not found with the dual-scatter technique. As shown in equation (A18), the Doppler frequency only depends on the angle between the input laser beams ϕ_2 and is thus independent of the finite acceptance angle of the lens. In order to reduce the instrument broadening error, the reference-scatter systems must use only a small portion of the collecting lens; however, the dual-scatter system, with no instrument broadening, may use as large a collecting lens as practical because, as seen from equation (A20), the contribution from the lens element outside the plane of the cross beams is of second order. As

shown later this difference is a major advantage of the dual-scatter technique.

Alignment problems developing from the complex receiver optical system in the single-beam technique constitute an undesirable trait. The cross-beam technique has simple optical systems that are easily aligned which, from this standpoint, makes the cross-beam system the more desirable LDV technique. Also, as shown in figures 2 and 3, the cross-beam system may be used in either the reference-scatter mode or the dual-scatter mode. Since the final analysis to determine the most efficient system is yet to be made, the single-beam system is not discussed further inasmuch as it is limited to only the reference-scatter mode and the characteristics of the reference-scatter mode are identical in the single-beam and cross-beam systems.

System Theory

Derivation of the Relation Between Signal-to-Noise Ratio and Scattered Laser Power

The instrumentation used to process the photomultiplier output current containing the Doppler frequency has input signal-to-noise and input power requirements. Since the power requirements may be met by using amplifiers, the signal-to-noise requirement is the limiting factor. Thus, a relation between signal-to-noise ratio and collected scattered light power must be determined.

If the reference-scatter mode is considered, there are two parallel and coaxial electromagnetic waves, the unscattered reference wave and the scattered signal wave, impinging upon the photocathode surface. Just before contact, the total wave may be described as the sum of the two waves as follows:

$$E_t = E_s \cos \omega_s t + E_r \cos \omega_r t \quad (1)$$

where E_t total wave

$E_s \cos \omega_s t$ signal wave

$E_r \cos \omega_r t$ reference wave

Since the photomultiplier is a square-law detector, the current $i(t)$ at its terminals is given by the equation

$$i(t) \propto E_t^2 = \frac{E_s^2 \cos^2 \omega_s t + E_r^2 \cos^2 \omega_r t + 2 E_s E_r \cos(\omega_s - \omega_r) t + 2 E_s E_r \cos(\omega_s + \omega_r) t}{2} \quad (2)$$

with 100 percent heterodyne efficiency assumed.

Taking a time average of equation (2), where the interval is short compared with the Doppler frequency but long compared with the optical frequencies, gives

$$i(t) = \beta \left(\frac{E_s^2}{2} + \frac{E_r^2}{2} + E_s E_r \cos(\omega_s - \omega_r) t \right) \quad (3)$$

where β is a proportionality constant of the photomultiplier. The photomultiplier is incapable of generating currents at optical frequencies $2\omega_s$, $2\omega_r$, and $\omega_s + \omega_r$, so these terms do not appear in the output. The output current is the sum of two components: the dc current $i_{dc}(t)$ and the Doppler frequency current $i_{if}(t)$ expressed as

$$i_{dc}(t) = \beta \left(\frac{E_s^2}{2} + \frac{E_r^2}{2} \right) \quad (4)$$

$$i_{if}(t) = \beta E_s E_r \cos(\omega_s - \omega_r) t \quad (5)$$

Thus, the Doppler frequency may be determined from the output of the photomultiplier.

To continue the derivation:

$$i(t) = \left(1 + \frac{i_{if}(t)}{i_{dc}(t)} \right) i_{dc}(t) \quad (6)$$

or

$$i(t) = \left(1 + \frac{2 E_s E_r \cos(\omega_s - \omega_r) t}{E_s^2 + E_r^2} \right) i_{dc}(t) \quad (7)$$

Thus

$$i_{if}(t) = \left(\frac{2 E_s E_r \cos(\omega_s - \omega_r) t}{E_s^2 + E_r^2} \right) i_{dc}(t) \quad (8)$$

The mean-square photodetector response $\langle i_{if}^2 \rangle$, where the brackets represent a time average over an interval of 1 Doppler frequency cycle, can then be computed from equation (8) and can be expressed as follows:

$$\langle i_{if}^2 \rangle = \frac{2 P_s P_r i_{dc}^2(t)}{(P_s + P_r)^2} \quad (9)$$

The noise sources for this system are considered to be composed of the dark current, shot noise, signal shot noise, background shot noise, and thermal noise (Johnson noise). Since the background light level can be controlled by the experimenter to a large degree, shot noise derived from the background light level is not considered in this paper. It can be shown that in normal LDV operation the signal shot noise will be at least two orders of magnitude greater than either dark current noise or Johnson noise. Therefore, it is assumed that this is the case in the present paper and that the total noise factor is due to signal shot noise only. Thus, the mean-square noise response $\langle i_n^2 \rangle$ in the detector is given by

$$\langle i_n^2 \rangle = 2 e \Delta f B g_p i_{dc}(t) \quad (10)$$

where e electron charge

Δf noise bandwidth

B statistical factor due to dynode emission of shot noise

g_p gain of photomultiplier

A signal-to-noise ratio is defined as

$$\frac{S}{N} = \frac{\langle i_{if}^2 \rangle}{\langle i_n^2 \rangle} = \frac{2 P_s P_r i_{dc}^2(t)}{2 (P_s^2 + 2 P_s P_r + P_r^2) e \Delta f B g_p i_{dc}(t)} \quad (11)$$

or

$$\frac{S}{N} = \frac{P_s P_r i_{dc}(t)}{(P_s^2 + 2 P_s P_r + P_r^2) e \Delta f B g_p} \quad (12)$$

but

$$e g_p = \frac{i_{dc}(t) h \nu}{(P_s + P_r) \eta}$$

(assuming complete photoelectron collection). Thus

$$S/N = \frac{\eta P_s P_r (P_s + P_r)}{(P_s^2 + 2 P_s P_r + P_r^2) \Delta f B h \nu} = \frac{\eta P_s P_r}{(P_s + P_r) \Delta f B h \nu} \quad (13)$$

where η quantum efficiency of photomultiplier

h Plancks constant

ν optical frequency of laser light

If P_r is kept much larger than P_s , equation (13) reduces to

$$S/N = \frac{\eta P_s}{h \nu \Delta f B} \quad (14a)$$

or, with S/N given in dB,

$$S/N_{dB} = 10 \log \frac{\eta P_s}{h \nu \Delta f B} \quad (14b)$$

In order to determine the ratio P_r/P_s when this condition applies, equation (13) is plotted with S/N as a function of P_r for a constant P_s . The constants in equation (13) for this test are based on a laser wavelength of 514.5 nm, an S-20 photomultiplier response, and a 1.0-MHz noise bandwidth. The resulting plots are given in figure 4. It may be seen that a P_r/P_s of 4 gives a signal-to-noise ratio within 1 dB of the maximum signal-to-noise ratio. Therefore, if the ratio P_r/P_s is kept at 4 or greater, then equation (13) will reduce to equation (14a).

If the dual-scatter system is considered with the optics located midway between the two laser beams, either forward-scatter or back-scatter, the signal wave and the reference wave will both be scattered waves and of equal power. Since $P_s = P_r$ in equation (13)

$$S/N = \frac{\eta P_s^2}{2 P_s h \nu \Delta f B} \quad (15)$$

or

$$S/N = \frac{\eta P_s}{2 h \nu \Delta f B} \quad (16a)$$

or, with S/N given in dB,

$$S/N_{db} = 10 \log \frac{\eta P_s}{2 h \nu \Delta f B} \quad (16b)$$

Thus the relationships between signal-to-noise ratio and scattered power have been developed for both the reference-scatter system and the dual-scatter system.

Rayleigh and Mie Scattering Functions

From classical electromagnetic theory, the scattering process is a function of the particle size relative to the wavelength of the impinging light and the optical characteristics of the material of the particles. In the case of scatter from molecules $2r < \lambda$ the theory has been developed by Rayleigh in reference 6. For particles on the order of the wavelength in size, the appropriate theory is given by Mie in reference 7.

If a laser beam is focused to a small sample volume, the scattered power received by the detector lens is given by the equation (ref. 5):

$$P_{sc} = F q (\sigma_r + \sigma_{Mie}) \Delta V \Omega \quad (17)$$

where $(\sigma_r + \sigma_{Mie})$ is the macroscopic scattering cross section per unit volume for Rayleigh scatter and Mie scatter, respectively. The factor q is the attenuation of the wave (transmissivity) in propagating from the scatterer to the detector lens. The quantity ΔV is the sample volume as determined by the volume common to the crossing laser beams. The factor Ω is the solid angle subtended by the receiving lens, and F is the laser power per unit area at the sample volume.

The macroscopic Rayleigh cross section for forward or back scatter is, as obtained from reference 6,

$$\sigma_r = \frac{(1 + \cos^2 \theta)}{2} k^4 \bar{\alpha}^2 N_r f \quad (18)$$

where k wave number of the incident radiation, $2\pi/\lambda$
 $\bar{\alpha}$ polarizability
 N_r molecular number density
 f depolarization attributable to the an isotropy of the scatterer, $\frac{3(2 + \Delta)}{6 - 7\Delta}$

- Δ depolarization factor
- θ angle of scattered light received by the viewing optics

Based on the assumption that the particulate matter present in the flow may be considered a collection of spherical particles of index of refraction n , the absolute Mie scattering cross section is given by the equation, as obtained from reference 7:

$$\sigma_{Mie} = \frac{1}{k^2} \sum_r i(\alpha_1, n, \theta) N_{Mie} \quad (19)$$

Where $i(\alpha_1, n, \theta)$ Mie intensity function, $\frac{i_{\perp}(\alpha_1, n, \theta) + i_{\parallel}(\alpha_1, n, \theta)}{2}$

$i_{\perp, \parallel}(\alpha_1, n, \theta)$ intensity of light with electric vector perpendicular and parallel to plane through direction of propagation of incident and scattered beams, respectively

(These intensity functions were calculated by using the computer program developed by McCormick in reference 5.)

α_1 particle size parameter, $2\pi r/\lambda$

N_{Mie} number density of particles at the sample volume

From equations (17), (18), and (19) the molecular and particulate number densities are related with the input laser power to the required scatter laser power.

Expansion of Basic Theory

In presenting the theory to obtain the criteria for the application of the laser Doppler velocimeter, consideration must be given to the limitations placed on the system by the input requirements for the processing instrumentation that will be used to condition the Doppler frequency signal. These requirements are a minimum signal-to-noise ratio and an input power range. Since the power may be adjusted by means of amplifiers or attenuators, the signal-to-noise ratio becomes the major requirement.

From equation (16b), the scattered laser power is related to the signal-to-noise ratio for the dual-scatter LDV. Solving for the scattered or signal power yields

$$P_s = \frac{2 h \nu \Delta f B 10^{\frac{S/N}{10}}}{\eta} \quad (20)$$

Taking the optical losses in the receiver into consideration gives

$$P_{sc} = \frac{P_s}{\epsilon} \quad (21)$$

where ϵ is the transmission coefficient of the receiver optics.

Equation (17) then relates the laser power scattered from the flow to the scattering functions and thus to the molecular and particle densities. This equation, repeated for the convenience of the reader, is

$$P_{sc} = F q (\sigma_r + \sigma_{Mie}) \Delta V \Omega \quad (17)$$

where F is the laser power density at the sample volume and is defined by

$$F = \frac{q P}{A_{CL}} \quad (22)$$

where q is the transmissivity of the medium and P is the input laser power. The cross-sectional area of the sample volume A_{CL} is defined

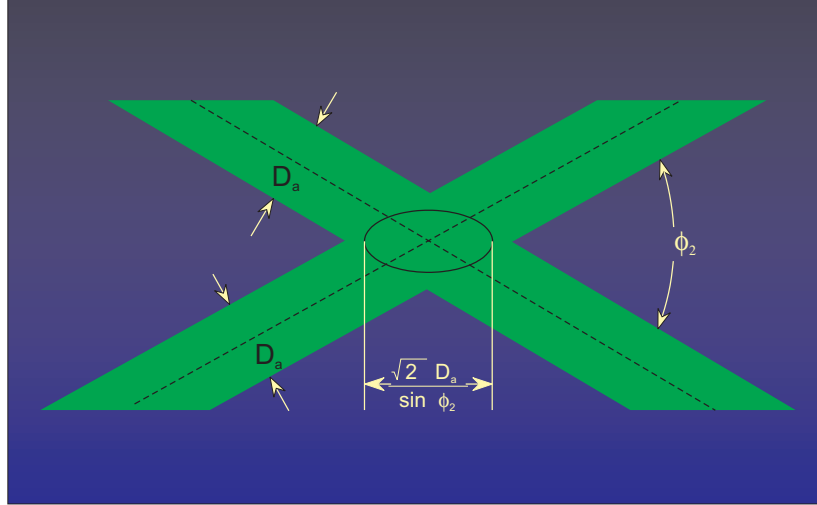
$$A_{CL} = \frac{\pi D_a^2}{4} \quad (23)$$

where D_a is the diameter of the sample volume and may be approximated by the Airy disk diameter (ref. 8), which is expressed as

$$D_a = \frac{1.22 \lambda F_1}{D} \quad (24)$$

where λ is the wavelength of light, F_1 is the input lens focal length, and D is the input aperture diameter.

The sample volume ΔV is in the form of an ellipsoid, shown in the following sketch, as described by the Airy disk diameter of the focused laser beam:



This volume may be determined by the Airy disk diameter of the focused laser beam as based on the input focusing lens and the sine of the angle between the two laser beams as

$$\Delta V = \frac{\pi D_a^3}{6 \sin \phi_2} \quad (25)$$

It is assumed that the entire sample volume is viewed by the receiving optics. If a larger volume is viewed by the receiving optics only the dc level will increase, with no change in spatial resolution with respect to the Doppler sample volume. This is because only scattered light from the beams scattering simultaneously from the same particle can combine in order to obtain the heterodyne effect.

The solid angle Ω viewed by the receiving optics is given by

$$\Omega = \frac{A_r}{Z^2} \quad (26)$$

where A_r is the area of the receiving lens and Z is the distance between the sample volume and the receiving lens. Thus the equations for determining the necessary criteria for application of a LDV system are known.

Application of Basic Theory

Development of a Computer Program

By programming the basic theory for the laser Doppler velocimeter, a design study may be made over a variety of physical parameters. Also, effects of instrument variations may be determined.

Consider a program that is to yield the necessary criteria for LDV operation in low-density wind tunnels, for example, a Mach 6 wind tunnel with a stagnation pressure of 4.14 MN/m^2 (600 psi) and a stagnation temperature of 204° C (400° F). With a closer look at the basic theory, it is found that for these conditions, if particles must be added to the flow in order to obtain the necessary scattered laser power, the molecular scattering contribution may be neglected. From appendix B, considering the example flow, the Rayleigh scattering cross section σ_r is $2.27 \times 10^{-7} \text{ m}^{-1}$. If 1 particle/cm³, with a particle diameter on the order of a micron, is added to the flow, the Mie scattering cross section σ_{Mie} is $1.7 \times 10^{-5} \text{ m}^{-1}$. For this condition the molecular scattering contribution may be neglected. For flows where the molecular densities are higher, this may not be the case. The molecular scattering results presented later give some approximation of the regions where molecular scattering must be considered.

The computer program containing the basic theory is presented in appendix C. In this program the contribution of scattered power due to molecular scatter has been neglected. The program as presented in appendix C is for the problem in which the required signal-to-noise ratio is an input and the minimum particle density necessary to obtain the required signal-to-noise ratio is determined. The LDV used in this case is the cross-beam dual-scatter system. The program will accept either forward-scatter or back-scatter problems. With a few modifications the program may be converted to handle a reference-scatter system. The program may also be converted for solving problems with particle density as an input and resultant signal-to-noise ratio determined.

Results of Application of the Program

The cross-beam system is the LDV considered. The system is used in the three modes of operation so that a comparison may be made between the modes. The modes are described as follows:

- (1) The dual-scatter-forward-scatter mode with the receiver lens located between the cross beams. The receiver lens is moved as the

cross-beam angle is varied in such a way that the lens just remains between the beams.

- (2) The dual-scatter-back-scatter mode with the input focusing lens used as the receiving lens.
- (3) The reference-scatter mode with the receiver located so that the distance between the sample volume and the receiving lens is the same as the lens distance for the dual-scatter-forward-scatter system with a cross-beam angle of 4° .

Each mode has its advantages as described previously. By the use of the program, a quantitative comparison is made of the modes as the cross-beam angle is varied from 1° to 8° . The cross beams for the dual-scatter modes will be of equal power whereas the cross beams for the reference-scatter mode will be 99 percent and 1 percent with the lower power beam used as the reference beam. The power ratio in the reference-scatter mode is used to obtain the reference-to-signal power ratio needed to maximize the signal-to-noise ratio as described previously. Also, by keeping the reference-beam power low, the photomultiplier is kept out of saturation.

In order to perform the calculations in the program, a few basic criteria must be fixed. For an example, the chosen criteria are

Laser: 1.0-W Argon at 514.5 nm (unless specified otherwise),
1.5-mm beam diameter

Input focusing lens focal length: 0.6096 m (24 in.)

Receiving lens diameter: 0.0762 m (3 in.)

Photomultiplier response: S-20

Photomultiplier gain: 8.0×10^4

Noise bandwidth: 10^6 Hz

The seeding particles are assumed to be uniformly distributed, having diameters from 0.4μ to 2.0μ , with an index of refraction of 1.48.

In figure 5, the sample volume is determined by the input focusing lens, which is the same for all three modes, as based on the Airy disk diameter. As is shown, the volume decreases as the angle between the cross beams increases. The length of the sample volume is given in figure 6. The sample-volume length also decreases with an increase in the angle

between the cross beams. Thus the spatial resolution of the LDV is determined as a function of cross-beam angle.

For the fixed inputs given, the signal-to-noise ratios, with a seeding particle density of $1000 \text{ particles/cm}^3$ and for cross-beam angles from 1° to 8° , have been computed. The plots for the three modes of operation are given in figure 7. Taking into consideration the placement of the receiver optics and the theoretical discussion, a closer examination of these plots may be made.

For a large signal-to-noise ratio, the dual-scatter-forward-scatter mode is found to be the best of the three modes. The primary reasons for the large signal-to-noise ratios and the shape of the curves may be found by referring to equations (A18), (16b), and (17) and figure 5. Equation (A18) states that the dual-scatter mode contains no instrument broadening; thus, a large receiving lens may be used, which allows a large viewing solid angle. By keeping the receiving lens just between the two beams, the solid angle viewed increases with increased cross-beam angle, which allows increased collection of scattered power. On the other hand, the sample volume decreases with an increase in cross-beam angle and thus limits the number of scattering centers. Also, the signal-to-noise ratio is less by a factor of two for the dual-scatter modes than for the reference-scatter mode. By taking these parameters into consideration in equation (17), the scattered power received by the receiving optics is determined. It can be seen in figure 7 that the solid angle increasing with increased cross-beam angle more than compensates for the loss of signal-to-noise ratio in equation (16b) and the decrease in sample volume. For example, the sample volume decreases by a factor of five with an increase in crossbeam angle from 1° to 5° , whereas the viewing solid angle increases by a factor of 25.

The dual-scatter-back-scatter mode has the same advantages and disadvantages as the dual-scatter-forward-scatter mode except that the viewing solid angle is fixed since the input lens is used as the receiving lens. This is the reason the curve decreases with increased cross-beam angle since the decreasing sample volume is the dominating factor in equation (17). Also, the Mie cross section is a factor of about 10 less in the back-scatter mode than in the forward-scatter mode, which reduces the signal-to-noise ratio and output power.

The low effective signal-to-noise ratio obtained from the reference-scatter mode is due to the fact that the useful viewing solid angle is determined by the reference-beam cross section at the receiving lens. Thus, the scattered power as determined by use of equation (17) is very low and decreases with the sample volume decrease for increased cross-beam angle. The scattered power is so low that the compensation due to

a more efficient signal-to-noise relation does not bring the effective signal-to-noise ratio up to the levels of the dual-scatter modes.

Figure 8 is obtained by performing calculations to determine photomultiplier output current based on LDV operation plotted in figure 7. These calculations are made by converting the input laser power to the photomultiplier from watts to photons/second and applying the following equation:

$$i(t) = N g_p e \eta \quad (27)$$

where	$i(t)$	photomultiplier output current, A
	N	number of photons per second impinging on the photocathode surface
	g_p	gain of the photomultiplier
	e	electron charge, C
	q	quantum efficiency of the photomultiplier for the laser wavelength

With the output current known, the output power may be determined for a 50-ohm characteristic impedance coaxial transmission line. With an output power in the form of dBm, the results for the three modes are compared in figure 9.

By working backwards with the signal-to-noise ratio as the input limit, the minimum particle density that will satisfy the instrument requirements (for example, 15 dB) may be calculated. The particle densities thus obtained are given in figure 10. On the basis of required minimum seeding particle density, the dual-scatter-forward-scatter mode is again the most favorable. In fact, it would seem from the curve that at a slightly larger cross-beam angle there would be enough scattered power from 1 particle/cm³ to obtain an acceptable signal-to-noise ratio. However, the signal obtained would be very intermittent and is not discussed further since a continuous output is assumed in this paper.

In figure 11 a comparison of the dual-scatter-forward-scatter mode and the reference-scatter mode is made for two different lasers, a 50-mW He/Ne and a 1.0-W Argon at 514.5 nm. It was found quite dramatically just how much more efficient the dual-scatter technique is than the reference-scatter technique since for a cross-beam angle above 2.5° the required particle density for the use of the dual-scatter mode with the

He/Ne laser is less, even up to a factor of 10, than the reference-scatter mode with the Argon laser.

For applications where it is impossible or undesirable to add seeding particles, it is worthwhile to consider the possibility of Rayleigh scattering from the molecules themselves. The computer program is now modified to handle molecular scattering parameters. The portion of the program containing the calculations for determining Mie scattering parameters is removed and replaced with the calculations for Rayleigh scatter. By using the most efficient LDV (the dual-scatter-forward-scatter system) with a cross-beam angle of 6° the input laser power requirements may be found for particular molecular densities (based on the 514.5 nm Argon line) that would satisfy the 15-dB signal-to-noise ratio in the example. The plots of molecular density as a function of input laser power are presented in figure 12 for three gases: helium, air, and carbon dioxide.

To illustrate laser wavelength dependence on Rayleigh scatter, consider the same test with air and vary the laser wavelength from 300.0 nm to 700.0 nm in steps of 50.0 nm. The results are given in figure 13 for an S-20 photomultiplier response. The most efficient response is around 350.0 nm. In order to determine the possibilities of using lasers currently available, figure 14 is presented to illustrate the same computation with specific laser wavelengths. The lasers used are

Argon (frequency doubled)	257.3 nm	ultraviolet
Helium-Cadmium	325.0 nm	ultraviolet
	441.6 nm	blue
Argon	488.0 nm	blue-green
	514.5 nm	green
Helium-Neon	632.8 nm	red
Ruby	694.3 nm	red

The CO_2 laser (wavelength, 10.6 μm) is in the infrared and is not detectable with the S-20 photomultiplier response.

It may be seen in figure 14 that the Helium-Cadmium laser is the most efficient, but at present the maximum power obtainable is about 50 mW, which is too low to be considered. The next most efficient is the Argon laser which does have the required output power in experimental lasers

that would satisfy the requirements for Rayleigh scattering of air with 1 atmosphere pressure at 23° C. The ruby laser also has the required output power even with its long wavelength, but it is a pulsed laser which does not allow continuous measurement of velocity.

Thus with a high-power Argon laser, the velocity of a gas flow of 1 atmosphere static pressure may be measured directly. If this is done, Brownian motion of the molecules must be taken into consideration when reducing the resulting data.

Determination of Operating Criteria for an LDV in a Test Flow

Consider a flow with a mean core velocity of 1200 m/s and a core diameter of 15 cm, with a 7.5-cm-thick boundary layer about the core. It is desirable to scan the velocity field in this flow. Thus the mean velocity range is 0 to 1200 m/s. A turbulence study is also desirable so that the final velocity scan will contain a turbulent velocity deviation about the mean velocity. In transposing the velocity measurements to Doppler frequency there will be a mean Doppler frequency representing the mean velocity, a Doppler frequency deviation representing the magnitude of the velocity deviation, and a rate or modulation of the Doppler frequency representing the rate at which the velocity changes. Thus the output Doppler frequency is analogous to an FM radio signal where the mean frequency is the FM carrier frequency, the deviation is the amplitude of the signal, and the modulation is the frequency of the signal carried by the carrier frequency.

The tunnel windows in this example are taken to be 4.0 cm in diameter and to be located along an axis perpendicular to the flow.

To begin the LDV design, the LDV restrictions previously used in the computer program will be adequate. The conditioning instrumentation used will be similar to the units used at the George C. Marshall Space Flight Center as discussed in reference 2. This instrumentation is based on a wide-band frequency tracker with automatic tracking and compression of signals. This tracker is considered in this example because it is typical of the readout instrumentation used with an LDV. The spectrum analyzer readout is not considered since it does not yield information that is readily reduced.

The frequency tracker requirements are

Input power: 0 dBm to -50 dBm

Input signal-to-noise ratio: greater than 15 dB (1-MHz noise bandwidth)

Frequency response: 5 MHz to 200 MHz

Frequency deviation: 0 to 50 percent of carrier frequency or 30 MHz, whichever is lower

Frequency modulation: 0 Hz to 100 KHz

Thus the LDV restrictions are complete.

Because of the window restriction of a 4.0-cm diameter, the greatest cross-beam angle that may be used is 7.5° for a flow diameter of 30 cm. The maximum cross-beam angle as restricted by the frequency response of the conditioning instrumentation may be calculated from equation (A18) which is

$$\Delta f_D = \frac{2V_s}{\lambda} \sin \frac{\phi_2}{2}$$

and can be written

$$\phi_2 = 2 \sin^{-1} \frac{\Delta f_D \lambda}{2V_s}$$

The mean velocity, 1200 m/s, may be measured with a 4.9° cross-beam angle. In order to allow for velocity fluctuation, the cross-beam angle is reduced to 4° .

With these two limitations the cross-beam-angle range is fixed. From the frequency response limitations of the conditioning instrumentation, the velocity ranges for the cross-beam-angle limits were determined from equation (A18) and are shown in the following table. The deviations shown in the table were determined by the conditioning instrumentation.

Cross-beam angle, ϕ_2 , deg	Minimum velocity, m/s		Maximum velocity, m/s	
	Mean	Deviation	Mean	Deviation
4	59	± 20	1254	± 220
7.5	30	± 10	668	± 118

Since the 4° cross-beam angle gives the largest velocity range, the remainder of the criteria are based on this angle.

From figure 5 it is found that the sample volume for this example is $1.25 \times 10^{-10} \text{ m}^3$. The length of the sample volume found in figure 6 is 5.2 mm. Thus the spatial resolution is determined. If a 1.0-W Argon laser is used, the required particle density is found from figure 10 to be 1500 particles/cm³ for the reference-scatter mode, 130 particles/cm³ for the dual-scatter-back-scatter mode, and about 7 particles/cm³ for the dual-scatter-forward-scatter mode.

In order to measure the velocity cross section of the flow, the LDV must be translated so that the sample volume, viewed by both the input and receiver lenses, moves across the flow. Since the dual-scatter-back-scatter mode has all components located on the same side of the tunnel, the system may be translated easier than the other modes. From all geometric and flow restrictions, the design engineer now knows the best LDV to use and the seeding requirements for that system.

Errors

When the LDV requirements are met and a system is installed in a test condition, several sources of error must be considered. Also, requirements must be altered slightly to satisfy noise sources neglected in this paper.

The accuracy of the final measurement is directly dependent upon the precision of the alignment of the LDV. In this consideration, errors may develop in the measurement of the angle between the cross beams, measurement of the laser-beam diameter entering the focusing lens, focal length of the lens, and location of the receiving lens. Although these errors are minor, a greater problem is found in that the spatial resolution is finite which can create large sources of error if the velocity

gradient at the sample point is large. For example, with a 4° cross-beam angle, the sample volume is 5.2 mm long which means that there is a 3.4-percent error about a center velocity of 760 m/s for a velocity gradient of 50 m/s/cm. Another source of error is the accuracy of the conditioning instrumentation used to process the Doppler frequency; as an example, the frequency tracker has a 3-percent inaccuracy of measurement.

The noise contributions that may be found are shot noise due to background light and noise introduced in the signal processing instrumentation. The net effect of including these sources of noise is to increase the level of the minimum detectable signal size.

Concluding Remarks

Two laser Doppler velocimeter (LDV) techniques, the single-beam and the cross-beam, have been described. The cross-beam system was shown to be the more versatile because it can be operated in three modes, the reference-scatter, the dual-scatter-forward-scatter, and the dual-scatter-back-scatter. Also, due to the simplicity of the cross-beam system it is easier to align than the single-beam system.

The basic theory for the calculation of the criteria for LDV operation was presented. A computer program incorporating the basic theory was also presented which allows the operating criteria to be determined easily for any LDV configuration described in this paper. The only parameters needed to make the calculations are tunnel and signal conditioning instrumentation requirements.

By presenting an example set of restricting parameters, a series of operating criteria were determined. These results show that the dual-scatter-forward-scatter mode of the cross-beam LDV is the most efficient of the three modes. Although not as efficient, the dual-scatter-back-scatter system has two advantages: (1) ease of translation since all components are located on the same side of the flow and (2) only one entrance window is required.

A typical design problem utilizing the techniques given in the paper is presented. The results obtained are the criteria necessary to obtain velocity measurements with the LDV. Thus, the design engineer may use the program to determine the optimum criteria for velocity measurement in a flow under study.

Langley Research Center,

National Aeronautics and Space Administration,

Hampton, Va., February 10, 1971.

APPENDIX A

Derivation of Doppler Frequency

Consider a small particle moving along a velocity vector V_s . If the particle radiates light energy and is viewed by a stationary observer located at a point along the velocity vector in front of the particle, the distance traveled by the light waves toward the observer in time t is $(c - V_s)t$. The number of light wavelengths emitted in this time is $f_s t$, where f_s is the frequency of the source. Therefore, the frequency seen by the observer f_o is expressed (ref.9)

$$f_o = \frac{c f_s t}{(c - V_s)t} = \frac{c f_s}{c - V_s} \quad (\text{A1})$$

However, if the light source is stationary and the observer is a particle moving away from the source, the frequency seen by the observer f_p is

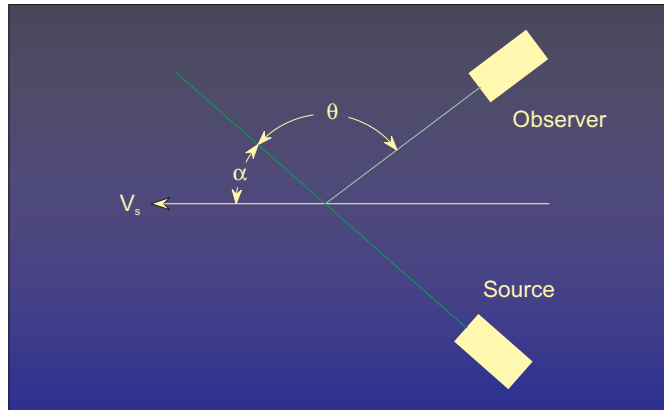
$$f_p = f_L \frac{c - V_s}{c} \quad (\text{A2})$$

If the source is not along the velocity vector, the frequency seen by the particle is given by

$$f_p = f_L \frac{c - V_s \cos \alpha}{c} \quad (\text{A3})$$

where α is the angle between the light beam and the velocity vector.

As light is scattered from the moving particle, it now becomes the source. With the observer located as shown in the following sketch, the observer will see the frequency f_D .



APPENDIX A

The frequency f_D can be written

$$f_D = \frac{c}{c - V_s \cos(\alpha + \theta)} f_p \quad (\text{A4})$$

Substituting for f_p in equation (A4) gives

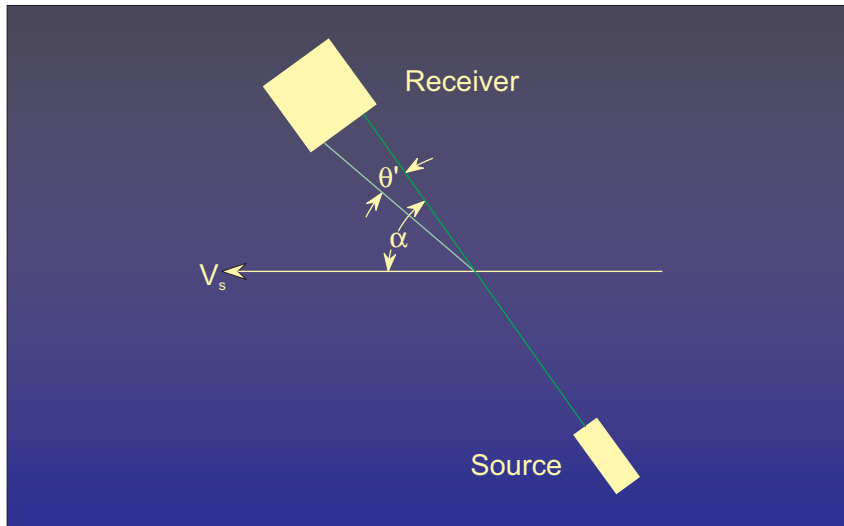
$$f_D = \frac{c - V_s \cos \alpha}{c} \frac{c}{c - V_s \cos(\alpha + \theta)} f_L \quad (\text{A5})$$

or

$$f_D = \frac{c - V_s \cos \alpha}{c - V_s \cos(\alpha + \theta)} f_L \quad (\text{A6})$$

Reference-Scatter LDV

If a reference-scatter system is used to determine the Doppler frequency, the angle relation is shown in the following sketch:



Note that $\cos(\alpha + \theta)$ in equation (A6) becomes $\cos(\alpha + \theta')$ where θ' is the angle between the observer optics and the reference beam. In the detector the two beams, the signal beam and the unscattered laser beam, are placed so that they are coaxial and parallel and impinge upon a photomultiplier where they heterodyne to yield the difference frequency between the light beams or the Doppler frequency.

APPENDIX A

In order to obtain the Doppler frequency Δf_D , the source frequency f_L is subtracted from both sides of equation (A6) to give

$$\Delta f_D = f_D - f_L = \frac{c - V_s \cos \alpha}{c - V_s \cos (\alpha - \theta')} f_L - f_L \quad (\text{A7})$$

or

$$\Delta f_D = \frac{c - V_s \cos \alpha - c + V_s \cos (\alpha - \theta')}{c - V_s \cos (\alpha - \theta')} f_L \quad (\text{A8})$$

But $c \gg V_s \cos(\alpha - \theta')$ for all velocities under consideration. Thus

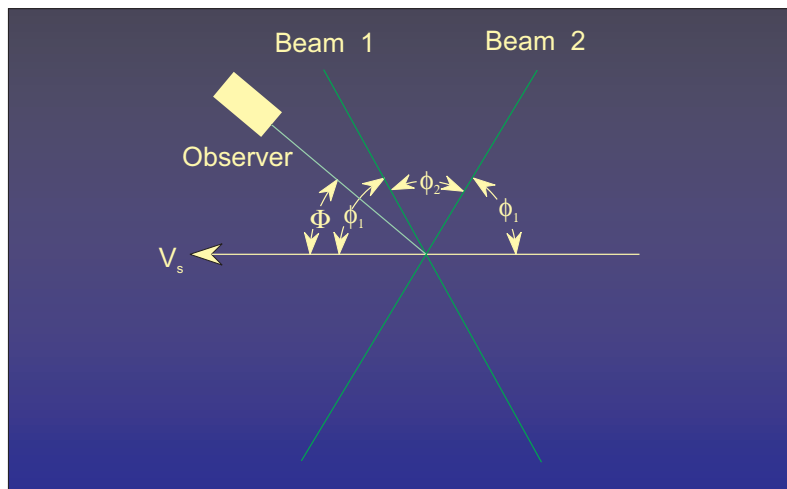
$$\Delta f_D = \frac{V_s}{\lambda} \left(\frac{\cos (\alpha - \theta') - \cos \alpha}{c} \right) \quad (\text{A9})$$

Therefore, the Doppler equation becomes

$$\Delta f_D = \frac{V_s}{\lambda} (\cos (\alpha - \theta') - \cos \alpha) \quad (\text{A10})$$

Dual-Scatter LDV

Now consider the dual-scatter system. If the observer is located as shown in the following sketch, the observer will collect scattered light from both beams.



APPENDIX A

If equation (A6) is applied to beam 1, the light frequency observed becomes

$$f_{D_1} = \frac{c - V_s \cos \alpha}{c - V_s \cos (\alpha + \theta)} f_L \quad (\text{A11})$$

where α and θ are redefined by the geometry as

$$\alpha = \phi_1 \quad \alpha + \theta = \Phi$$

Therefore

$$f_{D_1} = \frac{c - V_s \cos \phi_1}{c - V_s \cos \Phi} f_L \quad (\text{A12})$$

If equation (A6) is applied to beam 2, with α and θ redefined as

$$\alpha = \phi_1 + \phi_2 \quad \alpha + \theta = \Phi$$

the light frequency observed becomes

$$f_{D_2} = \frac{c - V_s \cos (\phi_1 + \phi_2)}{c - V_s \cos \Phi} f_L \quad (\text{A13})$$

The Doppler, or difference, frequency may then be found for the dual-scatter system by subtracting equation (A13) from equation (A12) to give

$$\Delta f_D = f_{D_1} - f_{D_2} = \frac{c - V_s \cos \phi_1}{c - V_s \cos \Phi} f_L - \frac{c - V_s \cos (\phi_1 + \phi_2)}{c - V_s \cos \Phi} f_L \quad (\text{A14})$$

or

$$\Delta f_D = \frac{f_L}{c - V_s \cos \Phi} (c - V_s \cos \phi_1 - c + V_s \cos (\phi_1 + \phi_2)) \quad (\text{A15})$$

But $c \gg V_s \cos \Phi$ for all velocities under consideration. Therefore

$$\Delta f_D = \frac{f_L V_s}{c} (\cos (\phi_1 + \phi_2) - \cos \phi_1) \quad (\text{A16})$$

APPENDIX A

Thus, the Doppler frequency is independent of the viewing angle of the observer for a dual-scatter system. This is not true for the reference-scatter system as shown in equation (A10).

Reducing the Doppler frequency to a more usable form yields

$$\Delta f_D = \frac{V_s}{\lambda} (\cos (\phi_1 + \phi_2) - \cos \phi_1) \quad (\text{A17})$$

For the case of symmetry, $\phi_1 = 90^\circ - \frac{\phi_2}{2}$

$$\begin{aligned} \Delta f_D &= \frac{V_s}{\lambda} \left(\cos \left(90^\circ - \frac{\phi_2}{2} + \phi_2 \right) - \cos \left(90^\circ - \frac{\phi_2}{2} \right) \right) \\ \Delta f_D &= -\frac{2 V_s}{\lambda} \cos \left(90^\circ - \frac{\phi_2}{2} \right) \\ \Delta f_D &= -\frac{2 V_s}{\lambda} \sin \frac{\phi_2}{2} \end{aligned} \quad (\text{A18})$$

Thus the Doppler frequency conversion factor

$$\frac{\Delta f_D}{V_s} = -\frac{2}{\lambda} \sin \frac{\phi_2}{2} \quad (\text{A19})$$

is only dependent upon the laser wavelength and the angle between the two input laser beams. Since it is desirable for the entire receiving lens to be used, the effect of collecting light out of the plane of the beams must be considered. The effect is found to be an additional cosine term in the denominator in equation (A15) so that the equation becomes

$$\Delta f_D = \frac{f_L}{c - V_s \cos \Phi \cos X} (c - V_s \cos \phi_1 - c + V_s \cos (\phi_1 + \phi_2)) \quad (\text{A20})$$

where X is the angle of scatter collected out of the plane of the laser beams.

Thus a similar assumption that $c \gg V_s \cos \Phi \cos X$ is still valid, which means that the Doppler frequency as described by equation (A19) is valid over the entire collecting lens.

APPENDIX B

Determination of the Effects of Rayleigh Scatter

In order to determine the contribution of Rayleigh scatter and Mie scatter to the total scattered laser power, these parameters are calculated for a typical wind tunnel. The wind tunnel used in this example is a Mach 6 wind tunnel with a stagnation pressure of 4.14 MN/m² (600 psi) and a stagnation temperature of 204° C (400° F). Based on the assumption that the flow is free of particulate material, only Rayleigh scatter from the molecules is considered.

Begin by determining the Rayleigh scattering cross section from equation (18), which is

$$\sigma_r = \frac{1 + \cos^2 \theta}{2} k^4 \bar{\alpha}^2 N_r f \quad (18)$$

where	k	wavenumber, $2\pi/\lambda$ or 1.22×10^7
	$\bar{\alpha}$	polarizability of air, $1.79 \times 10^{-30} \text{ m}^3$
	N_r	molecular density, $3.04 \times 10^{24} \text{ molecules/m}^3$
	f	depolarization factor (ref. 5), 1.054
	θ	viewing angle of scattered light, 4°

The result is $\sigma_r = 2.27 \times 10^{-7} \text{ m}^{-1}$.

In order to determine the effect of added particles, seed the flow with particles in a uniform distribution from 0.4 μ to 2.0 μ in diameter so that the particle concentration is 1 particle/cm³. The Mie scattering cross section is found from equation (19) which is

$$\sigma_{Mie} = \frac{1}{k^2} \sum_r i(\alpha_1, n, \theta) N_{Mie} \quad (19)$$

The result is $\sigma_{Mie} = 1.7 \times 10^{-5} \text{ m}^{-1}$.

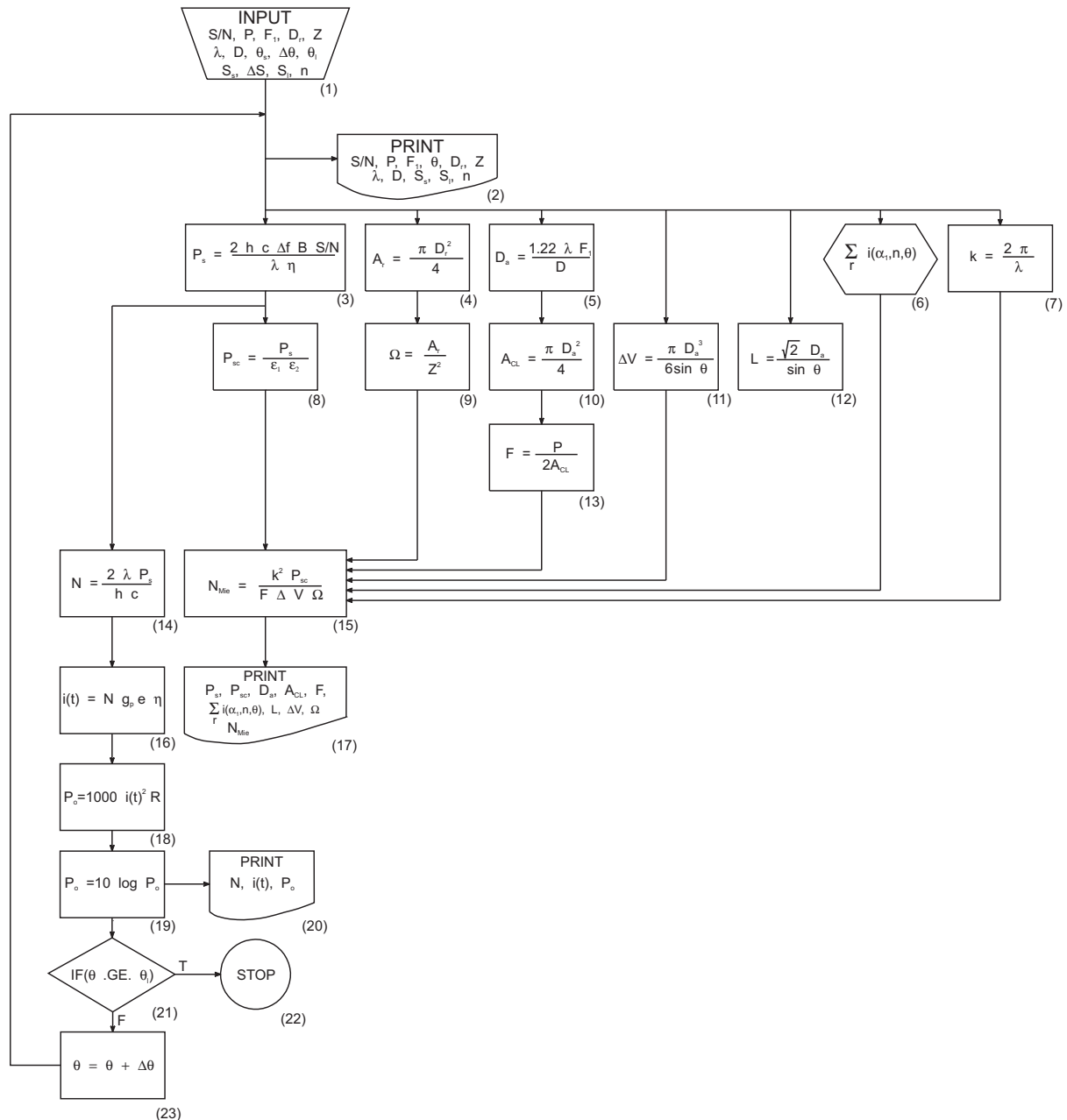
APPENDIX B

When the Mie scattering cross section is compared to the Rayleigh scattering cross section it is seen that the Rayleigh scattering cross section can be neglected if the particle concentration is 1 particle/cm³ or greater if the molecular density is 3.04×10^{24} molecules/m³ or less. If higher molecular densities are in the flow, this may not be the case and these calculations must be performed to determine the contribution of each scattering cross section.

APPENDIX C

Computer Program For Calculation of LDV Parameters

The organization of the computer program used to obtain the required parameters for a given LDV configuration is illustrated in the following flow chart:



APPENDIX C

A detailed explanation of the numbered blocks in the flow chart is as follows:

Block 1: Input parameters needed

$(S/N)_{\text{dB}}$	signal-to-noise ratio, dB
P	input laser power, W
F_i	input lens focal length, m
D_r	diameter of receiving lens, m
Z	distance from sample volume to receiving lens, m
λ	wavelength of laser beam, m
D	diameter of input aperture, m
θ_s	starting cross-beam angle, deg
$\Delta\theta$	incremental cross-beam angle, deg
θ_l	final cross-beam angle, deg
S_s	starting particle diameter, microns
ΔS	incremental particle diameter, microns
S_l	final particle diameter, microns
n	index of refraction of particles

Block 2: Printed output of input parameters

Block 3: Calculation of the required scattered power impinging on the photomultiplier to satisfy the input signal-to-noise parameter from equation (20)

$$P_s = \frac{2 h c \Delta f B 10^{\frac{S/N}{10}}}{\lambda \eta} \quad (20)$$

APPENDIX C

where	h	Plancks constant, 6.626×10^{-34} J-s
	c	velocity of light, 3×10^8 m/s
	Δf	noise bandwidth, 10^6 Hz
	B	statistical factor due to dynode emission of shot noise, 1.2
	η	quantum efficiency of the photomultiplier, 0.13 for 514.5 nm laser wavelength and S-20 response

Block 4: Calculation of the area of the receiving lens

$$A_r = \frac{\pi D_r^2}{4} \quad (C1)$$

Block 5: Calculation of the Airy disk diameter as based on the input focusing lens by use of equation (24)

$$D_a = \frac{1.22 \lambda F_1}{D} \quad (24)$$

Block 6: Subroutine to calculate the Mie intensity function for a uniform distribution of particle size as given in the input parameters.

Block 7: Calculation of the wave number

$$k = \frac{2\pi}{\lambda} \quad (C2)$$

Block 8: Calculation of scattered power required from the flow (eq. (17))

$$P_{sc} = \frac{P_s}{\epsilon} = \frac{P_s}{\epsilon_1 \epsilon_2} \quad (17)$$

where	ϵ_1	percent transmission of light through receiving lens, 0.92
	ϵ_2	percent transmission of light through beam splitter, 0.45

APPENDIX C

Block 9: Calculation of viewing solid angle by use of equation (26)

$$\Omega = \frac{A_r}{Z^2} \quad (26)$$

Block 10: Calculation of cross-sectional area of the sample volume by use of equation (23)

$$A_{CL} = \frac{\pi D_a^2}{4} \quad (23)$$

Block 11: Calculation of sample volume by use of equation (25)

$$\Delta V = \frac{\pi D_a^3}{6 \sin \theta} \quad (25)$$

Block 12: Calculation of the length of the sample volume

$$L = \frac{1.414 D_a}{\sin \theta} \quad (C3)$$

Block 13: Calculation of laser power density at sample volume

$$F = \frac{P}{2 A_{CL}} \quad (C4)$$

The factor of 2 is included because of the division of the input laser beam into two crossing beams for the dual-scatter system

Block 14: Calculation of number of photons per second impinging upon the photocathode surface

$$N = \frac{2 \lambda P_s}{h c} \quad (C5)$$

Block 15: Calculation of the required number density to satisfy the input parameters

$$N_{Mie} = \frac{k^2 P_{sc}}{F \Delta V \Omega \sum_r i(\alpha_1, n, \theta)} \quad (C6)$$

APPENDIX C

Block 16: Calculation of output current from the photomultiplier by use of equation (27)

$$i(t) = N g_p e \eta \quad (27)$$

Block 17: Printed output of calculated parameters

P_s	required scatter power
P_{sc}	scattered power required from flow
D_a	Airy disk diameter
A_{CL}	cross-sectional area of sample volume
F	laser power density at sample volume
$\sum_r i(\alpha_1, n, \theta)$	Mie intensity function
L	length of sample volume
ΔV	sample volume
Ω	viewing solid angle
N_{Mie}	required particle density

Block 18: Calculation of output power from the photomultiplier

$$P_o = 1000 i^2(t) R \quad (C7)$$

where R output impedance of matching unity gain amplifier, 50 ohms

(The 1000 is a conversion from watts to milliwatts.)

Block 19: Conversion of output power to output power in dBm

Block 20: Printed output of calculated parameters

N	number of photons per second impinging on the photocathode surface
$i(t)$	output current from photomultiplier

APPENDIX C

P_o output power from photomultiplier

Block 21: IF statement to determine whether scattering-angle scan is complete

Block 22: Scattering-angle scan is complete; STOP

Block 23: Scattering-angle scan is not complete; increment angle and go to input

A printout of the program is given on the following pages.

APPENDIX C

```
PROGRAM LASER(INPUT,OUTPUT,TAPE5=INPUT,TAPE6=OUTPUT,TAPE9)
DIMENSION SREF(2)
```

```
C      THE PROGRAM WILL CALCULATE THE REQUIRED PARTICLE DENSITY, AND
C      OUTPUT PARAMETERS FOR A DUAL SCATTER TYPE LASER DOPPLER VELOCIMETER
C      (LDV).  THE LDV MAY BE IN EITHER FORWARD SCATTER MODE OR BACK SCATTER
C      MODE, WHERE FORWARD SCATTER CONTAINS ANGLES FROM 0.0 DEGREES TO 90.0
C      DEGREES, AND BACK SCATTER CONTAINS ANGLES FROM 90.0 DEGREES TO 180.0
C      DEGREES.  THE INPUT PARAMETERS NEEDED ARE, SIGNAL-TO-NOISE RATIO AT
C      THE PHOTOMULTIPLIER, INPUT LASER POWER, FOCAL LENGTH OF INPUT
C      FOCUSING LENS, RECEIVER LENS DIAMETER, DISTANCE FROM SAMPLE VOLUME
C      TO RECEIVING LENS, LASER WAVELENGTH, LASER BEAM DIAMETER, STARTING
C      CROSS BEAM ANGLE, INCREMENT ANGLE, AND FINAL ANGLE, PARTICLE
C      DISTRIBUTION AND INDEX OF REFRACTION.
```

```
C      THE OUTPUT CONTAINS THE SIZE OF THE SAMPLE VOLUME, SCATTERED
C      LIGHT POWER RECEIVED, MIE INTENSITY FUNCTION, REQUIRED PARTICLE
C      DENSITY AND PHOTOTUBE OUTPUT CURRENT AND POWER.
```

```
C      SN = REQUIRED SIGNAL-TO-NOISE RATIO IN DB.
C      P0 = INPUT LASER POWER IN WATTS
C      F1 = FOCAL LENGTH OF INPUT LENS IN METERS.
C      DR = DIAMETER OF RECEIVING LENS IN METERS.
C      Z = DISTANCE FROM SAMPLE VOLUME TO RECEIVING LENS IN METERS.
C      XLAM = LASER WAVELENGTH IN METERS.
C      D = INPUT LASER DIAMETER IN METERS.
C      DTHETA = STARTING CROSS BEAM ANGLE IN DEGREES.
C      DETH = INCREMENT CROSS BEAM ANGLE IN DEGREES.
C      DTHELA = ENDING CROSS BEAM ANGLE IN DEGREES.
C      S = STARTING PARTICLE DIAMETER IN MICRONS.
C      DELTA = INCREMENT PARTICLE DIAMETER IN MICRONS.
C      SLAST = ENDING PARTICLE DIAMETER IN MICRONS.
C      SREF = PARTICLE INDEX OF REFRACTION.
```

```
READ 1, SN, P0, F1, DR, Z
READ 2, XLAM, D
READ 3, DTHETA, DETH, DTHELA
READ 3, S, DELTA, SLAST
```

```
READ 3, SREF
1 FORMAT (F15.6)
2 FORMAT (E15.6)
3 FORMAT (3F10.8)
SN9 = SN
```

APPENDIX C

```
S9 = S
DELTA9 = DELTA
SLAST9 = SLAST
P = P0/2.0
1000 SN = SN9
S = S9
DELTA = DELTA9
SLAST = SLAST9
PRINT 100
100 FORMAT (1H1,20X, *LDV DUAL SCATTER MODE, INPUT S/N*////)
PRINT 10
PRINT 11, SN
PRINT 12, P0
PRINT 13, F1
PRINT 14, DTHETA
PRINT 15, DR
PRINT 16, Z
PRINT 17, XLAM
PRINT 18, D
PRINT 19, S, SLAST
PRINT 20, SREF
THETA = DTHETA*0.01745329252
PIM = 3.14159E-06
S = PIM*S/XLAM
DELTA = PIM*DELTA/XLAM
SLAST = PIM*SLAST/XLAM
H = 6.626E-34
C = 3.0E08
DELF = 1.0E06
B = 1.2
E = 1.6E-19
G = 8.0E+04
XNU = 0.05
EL1 = 0.92
EL2 = 0.45
R = 50.0
SN = SN/10.0
XN = 10.0**SN
C CALCULATION OF REQUIRED SCATTERED POWER GOING TO PHOTOTUBE
PS = 2.0*H*C*DELF*B*SN/(XLAM*XNU)
PRINT 21
PRINT 22, PS
C CALCULATION OF REQUIRED SCATTERED POWER
```

APPENDIX C

```
PSC = PS/(EL1*EL2)
PRINT 23, PSC
C   CALCULATION OF INPUT POWER DENSITY
DA = 1.22*XLAM*F1/D
PRINT 24, DA
ACL = 3.14159*DA*DA/4.0
PRINT 25, ACL
F = P/ACL
PRINT 26, F
C   CALCULATION OF MIE INTENSITY FUNCTION
CALL MIEAB(S, DELTA, SLAST, SREF)
AASUM = 0.0
COUNT = 0.0
IF (DTHETA.GT.90.0) GO TO 201
DTHETA = DTHETA/2.0
GOTO 210
201 DTHETA = 180.0 - DTHETA
DTHETA = DTHETA/2.0
DTHETA = 180.0 - DTHETA
210 CONTINUE
CALL MIEAC(DTHETA, AASUM, COUNT)
XIMIE = AASUM/COUNT
IF (DTHETA.GT.90.0) GO TO 202
DTHETA = DTHETA*2.0
GO TO 211
202 DTHETA = 180.0 - DTHETA
DTHETA = DTHETA*2.0
DTHETA = 180.0 - DTHETA
211 CONTINUE
PRINT 27, XIMIE
C   CALCULATION OF SAMPLE VOLUME
XL = 1.414214*DA*COS(THETA/2.0)/SIN(THETA)
PRINT 34, XL
V = 3.14159*DA*DA*DA*COS(THETA/2.0)*SIN(THETA/2.0)/(3.0*SIN(THETA)
1*SIN(THETA))
PRINT 33, V
C   CALCULATION OF SOLID ANGLE
AR = 3.14159*DR*DR/4.0
OMEGA = AR/(Z*Z)
PRINT 28, OMEGA
C   CALCULATION OF REQUIRED PARTICLE DENSITY
XK = 2.0*3.14159/XLAM
XNMIE = XK*XK*PSC/(F*V*OMEGA*XIMIE)
```

APPENDIX C

```
XNMIE = XNMIE/10.0**6
PRINT 29, XNMIE
C CALCULATION OF OUTPUT POWER
P1 = 2.0*PS
XN = XLAM*P1/(H*C)
PRINT 30, XN
XIOUT = XN*G*E*XNU
XIOUT = XIOUT*0.5857
PRINT 31, XIOUT
XPOUT = XIOUT*XIOUT*R*1000.0
XPOUT = 10.0*ALOG10(XPOUT)
PRINT 32, XPOUT
IF(DTHETA.GE.DTHELA) GO TO 200
DTHETA = DTHETA + DETH
IF (DTHETA.GT.90.0) GO TO 220
THETA2 = DTHETA*0.01745329252/2.0
Z = DR/(2.0*TAN(THETA2))
GO TO 230
220 Z = F1
230 CONTINUE
GO TO 1000
200 CONTINUE
10 FORMAT (20X, * INPUT PARAMETERS*//)
11 FORMAT (* SIGNAL-TO-NOISE RATIO ----*F10.4* DB*/)
12 FORMAT (* LASER POWER ----*F10.4* WATTS*/)
13 FORMAT (* INPUT LENS FOCAL LENGTH ----*F10.4* METERS*/)
14 FORMAT (* SCATTERING ANGLE ----*F10.4* DEGREES*/)
15 FORMAT (* COLLECTING LENS DIAMETER ----*F10.4* METERS*/)
16 FORMAT (* DISTANCE FROM SAMPLE VOLUME TO COLLECTING LENS ----*
1 F10.4* METERS*/)
17 FORMAT (* LASER WAVELENGTH ----*E15.6* METERS*/)
18 FORMAT (* DIAMETER OF INPUT LASER BEAM ----*E15.6* METERS*/)
19 FORMAT (* PARTICLE RANGE ----*F8.4* MICRONS TO *F8.4* MICRONS*/)
20 FORMAT (* INDEX OF REFRACTION OF THE PARTICLES ----*F10.4* + J*
1 F10.4////)
21 FORMAT (20X, * OUTPUT PARAMETERS*//)
22 FORMAT (* SCATTERED POWER RECEIVED BY PHOTOMULTIPLIER ----*E15.6
2 * WATTS*/)
23 FORMAT (* SCATTERED POWER REQUIRED FROM FLOW ----*E15.6* WATTS*/)
24 FORMAT (* AIRY DISK DIAMETER ----*E15.6* METERS*/)
25 FORMAT (* CROSS SECTIONAL AREA OF SAMPLE VOLUME ----*E15.6
3 * SQMETERS*/)
26 FORMAT (* LASER POWER DENSITY AT SAMPLE VOLUME ----*E15.6
```

APPENDIX C

```
4 * WATTS/SQMETER*/)
27 FORMAT (* MIE INTENSITY FUNCTION ----*E15.6/)
28 FORMAT (* SOLID ANGLE OF THE VIEWING OPTICS ----*E15.6* SR*/)
29 FORMAT (* REQUIRED PARTICLE DENSITY ----*E15.6* PARTICLES/CC*/)
30 FORMAT (* INPUT POWER TO PHOTOMULTIPLIER ----*E15.6* PHOTONS/SEC*/
5 )
31 FORMAT (* PHOTOMULTIPLIER OUTPUT CURRENT ----*E15.6* AMPS*/)
32 FORMAT (* PHOTOMULTIPLIER OUTPUT POWER ----*F10.4* DBM*////)
33 FORMAT (* SAMPLE VOLUME ----*E15.6* CUBMETERS*/)
34 FORMAT (* LENGTH OF THE SAMPLE VOLUME ----*E15.6* METERS*/)
STOP
END

SUBROUTINE MIEAB(S, DELTA, SLAST, SREF)
C MIE A AND B MAIN PROGRAM
DIMENSION SREF(2), WN(2), WNM1(2), WNM2(2), ALAST(2), ANEXT(2), REF(2), A
$ (2), B(2)
COMMON REF, X, A, B, FN, WN, WNM1, WNM2, ALAST, ANEXT
INTEGER ZERO1
ZERO1=0
LUN=9
1101 CONTINUE
CALL RECOU(LUN, 1, 0, ZERO1, A(1), A(2), B(1), B(2))
CALL RECOU(LUN, 1, 0, S, SREF(1), SREF(2))
C INITIALIZATION
101 FN=0.0
TEST=1.2*S+9.
X=S
WN(1)=SIN(X)
WN(2)=COS(X)
WNM1(1)=WN(2)
WNM1(2)=-WN(1)
REF(1)=SREF(1)
REF(2)=SREF(2)
U=REF(1)*X
V=-REF(2)*X
SU=SIN(U)
CU=COS(U)
W=EXP(V)
W1=1./W
SHV=0.5*(W-W1)
CHV=0.5*(W+W1)
```

APPENDIX C

```
      TEM1=1./ (SU*SU+SHV*SHV)
      ANEXT(1)=SU*CU*TEM1
      ANEXT(2)=SHV*CHV*TEM1
C     STEP UP FOR NEXT CALCULATION
      3 ALAST(1)=ANEXT(1)
      ALAST(2)=ANEXT(2)
      WNM2(1)=WNM1(1)
      WNM2(2)=WNM1(2)
      WNM1(1)=WN(1)
      WNM1(2)=WN(2)
      FN=FN+1.
C     COMPUTE A AND B
      CALL NEXTAB
      N=FN
      CALL RECOUT(LUN,1,0,N,A(1),A(2),B(1),B(2))
      IF(FN.GE.TEST) GO TO 9
      IF((ABS(A(1)).GT.1.E-8).OR.(ABS(A(2)).GT.1.E-8).OR.(ABS(B(1))
      1 .GT.1.E-8).OR.(ABS(B(2)).GT.1.E-8)) GO TO 3
      9 IF(S.GE.SLAST) GO TO 10
      12 S=S+DELTA
      GO TO 1101
      10 CONTINUE
      700 CALL RECOUT(LUN,1,0,ZERO1,A(1),A(2),B(1),B(2))
      END FILE 9
      901 REWIND 9
      RETURN
      END

      SUBROUTINE NEXTAB
      DIMENSION WN(2),WNM1(2),WNM2(2),ALAST(2),ANEXT(2),REF(2),A(2),B(2)
      DIMENSION STORE1(2),STORE2(2),ADENOM(2),BDENOM(2),ANUM(2),BNUM(2)
      COMMON REF,X,A,B,FN,WN,WNM1,WNM2,ALAST,ANEXT
C     CALCULATE NEXT A+B FROM LAST
      DEN1=(REF(1)*REF(1)+REF(2)*REF(2))*X
      TERM1=FN/DEN1
      TERM2=TERM1*REF(2)
      TERM1=-TERM1*REF(1)
      DENOM1=-TERM1-ALAST(1)
      DENOM2=-TERM2-ALAST(2)
      TEMP=1./ (DENOM1*DENOM1+DENOM2*DENOM2)
      ANEXT(1)=TERM1+DENOM1*TEMP
      ANEXT(2)=TERM2-DENOM2*TEMP
```

APPENDIX C

```
FACT=(2.*FN-1.)/X
WN(1)=FACT*WNM1(1)-WNM2(1)
WN(2)=FACT*WNM1(2)-WNM2(2)
STORE=FN/X
CALL DIVCPX(ANEXT,REF,STORE1)
STORE1(1)=STORE1(1)+STORE
CALL MPYCPX(STORE1,WN,STORE2)
CALL SUBCPX(STORE2,WNM1,ADENOM)
ANUM(1)=WN(1)*STORE1(1)
ANUM(2)=WN(1)*STORE1(2)
ANUM(1)=ANUM(1)-WNM1(1)
CALL DIVCPX(ANUM,ADENOM,A)
CALL MPYCPX(ANEXT,REF,STORE1)
STORE1(1)=STORE1(1)+STORE
CALL MPYCPX(STORE1,WN,STORE2)
CALL SUBCPX(STORE2,WNM1,BDENOM)
BNUM(1)=WN(1)*STORE1(1)
BNUM(2)=WN(1)*STORE1(2)
BNUM(1)=BNUM(1)-WNM1(1)
CALL DIVCPX(BNUM,BDENOM,B)
RETURN
END
```

```
SUBROUTINE DIVCPX(X,Y,Z)
DIMENSION X(2),Y(2),Z(2)
DENOM=Y(1)*Y(1)+Y(2)*Y(2)
Z1=(X(1)*Y(1)+X(2)*Y(2))/DENOM
Z2=(X(2)*Y(1)-X(1)*Y(2))/DENOM
Z(1)=Z1
Z(2)=Z2
RETURN
END
```

```
SUBROUTINE MPYCPX(X,Y,Z)
DIMENSION X(2),Y(2),Z(2)
Z1=X(1)*Y(1)-X(2)*Y(2)
Z2=X(1)*Y(2)+X(2)*Y(1)
Z(1)=Z1
Z(2)=Z2
RETURN
END
```

APPENDIX C

```
SUBROUTINE SUBCPX(X,Y,Z)
DIMENSION X(2),Y(2),Z(2)
Z(1)=X(1)-Y(1)
Z(2)=X(2)-Y(2)
RETURN
END

SUBROUTINE MIEAC(DTHETA, AASUM, COUNT)
C PROGRAM TO CALC. QE, QS, AND I(180) USING DEIRMENDJIAN-S A-S AND B-
C
DIMENSION A(500,2),B(500,2),M(500),PI(500),TAU(500)
C
1000 I=1
LUN=9
THETA=DTHETA*0.017453292519943
STHETA=SIN(THETA)
STHESQ=STHETA**2
CTHETA=COS(THETA)
CTHESQ=CTHETA**2
PI(1)=1.0
PI(2)=3.*CTHETA
TAU(1)=CTHETA
TAU(2)=3.*(CTHESQ-STHESQ)
CALL RECIN(LUN,1,0,M(I),A(I,1),A(I,2),B(I,1),B(I,2))
5 CALL RECIN(LUN,1,0,ALPHA,ETAR,ETAI)
IF(EOF,9) 901,1
1 DO 2 II=1,250
I=II
CALL RECIN(LUN,1,0,M(I),A(I,1),A(I,2),B(I,1),B(I,2))
IF(M(I)) 2,3,2
2 CONTINUE
3 CONTINUE
MAX=I-1
SUM1=0.0
SUM2=0.0
C=-1.0
DO 11 I=1,MAX
XI=I
SUM1=(2.*XI+1.0)*(A(I,1)+B(I,1))+SUM1
SUM2=(2.*XI+1.0)*(A(I,1)**2+A(I,2)**2+B(I,1)**2+B(I,2)**2)+SUM2
11 CONTINUE
QE=2.0*SUM1/(ALPHA**2)
```

APPENDIX C

```
QS=2.0*SUM2/(ALPHA**2)
IF(DTHETA.NE.180.) GO TO 12
SUM4=0.0
SUMRE=0.0
SUMIM=0.0
DO 4 I=1,MAX
C=C*(-1.0)
XI=I
SUMRE=(XI+0.5)*(A(I,1)-B(I,1))*C+SUMRE
SUMIM=(XI+0.5)*(A(I,2)-B(I,2))*C+SUMIM
4 CONTINUE
SQMGRE=SUMRE*SUMRE
SQMGIM=SUMIM*SUMIM
SUM3=SQMGRE+SQMGIM
GO TO 30
12 CONTINUE
DO 13 NN=3,MAX
XN=NN
TWNM1=2.*XN-1.
PI(NN)=(TWNM1*PI(NN-1)*CTHETA-XN*PI(NN-2))/(XN-1.)
TAU(NN)=CTHETA*(PI(NN)-PI(NN-2))-(TWNM1)*STHESQ*PI(NN-1)+TAU(NN-2
1 )
13 CONTINUE
SSSR1=0.0
SSSI1=0.0
SSSR2=0.0
SSSI2=0.0
DO 14 NN=1,MAX
XN=NN
TEMP=(2.*XN+1.)/(XN*(XN+1.))
TEMPPI=TEMP*PI(NN)
TEMPTAU=TEMP*TAU(NN)
SSSR1=TEMPPI*A(NN,1)+TEMPTAU*B(NN,1)+SSSR1
SSSI1=TEMPPI*A(NN,2)+TEMPTAU*B(NN,2)+SSSI1
SSSR2=TEMPTAU*A(NN,1)+TEMPPI*B(NN,1)+SSSR2
SSSI2=TEMPTAU*A(NN,2)+TEMPPI*B(NN,2)+SSSI2
14 CONTINUE
SUM3=SSSR1**2+SSSI1**2
SUM4=SSSR2**2+SSSI2**2
AASUM=SUM4+AASUM
COUNT=COUNT+1.0
30 CONTINUE
GO TO 5
```

APPENDIX C

C

```
901 CONTINUE
700 CONTINUE
  REWIND 9
  RETURN
  END
```

```
15.0
0.05
0.6096
0.0762
4.366
  6328000E-07
  2000000E-03
170.0      0.25      179.0
0.4        0.005     2.0
1.48
```

References

1. Foreman, J. W., Jr.; George, E. W.; and Lewis, R. D.: *Measurement of Localized Flow Velocities in Gases With a Laser Doppler Flowmeter*. Appl. Phys. Lett., vol. 7, no. 4, Aug. 15, 1965, pp. 77-78.
2. Huffaker, Robert M.; Fuller, Charles E.; and Lawrence, T. R.: *Application of Laser Doppler Velocity Instrumentation to the Measurement of Jet Turbulence*. [Preprint] 690266, Soc. Automot. Eng., Jan. 1969.
3. Lennert, A. E.; Brayton, D. B.; Goethert, W. H.; and Smith, F. H.: *Laser Applications for Flow Field Diagnostics*. Laser J., vol. 2, no. 2, Mar/Apr. 1970, pp. 19-27.
4. Semat, Henry; and Katz, Robert: **Physics**. Rinehart & Co., Inc., c.1958.
5. McCormick, Michael Patrick: *Laser Backscatter Measurements of the Lower Atmosphere*. Ph. D. Thesis, Coll. of William and Mary in Virginia, 1967.
6. Born, Max; and Wolf, Emil: **Principles of Optics**. Third ed., Pergamon Press, c.1965.
7. Lennert, A. E.; Brayton, E. B.; Crosswy, F. L.; et al.: *Summary Report of the Development of a Laser Velocimeter To Be Used in AEDC Wind Tunnels*. AEDC-TR-70-101, U.S. Air Force, July 1970.
8. Rayleigh, (Lord): *On the Light From the Sky, Its Polarization and Colour*. Scientific Papers, Vol. I, Cambridge Univ. Press, 1899, pp. 87-103.
9. Mie, G.: *Optics of Turbid Media*. Ann. Phys., vol. 25, no. 3, 1908, pp. 377-445.

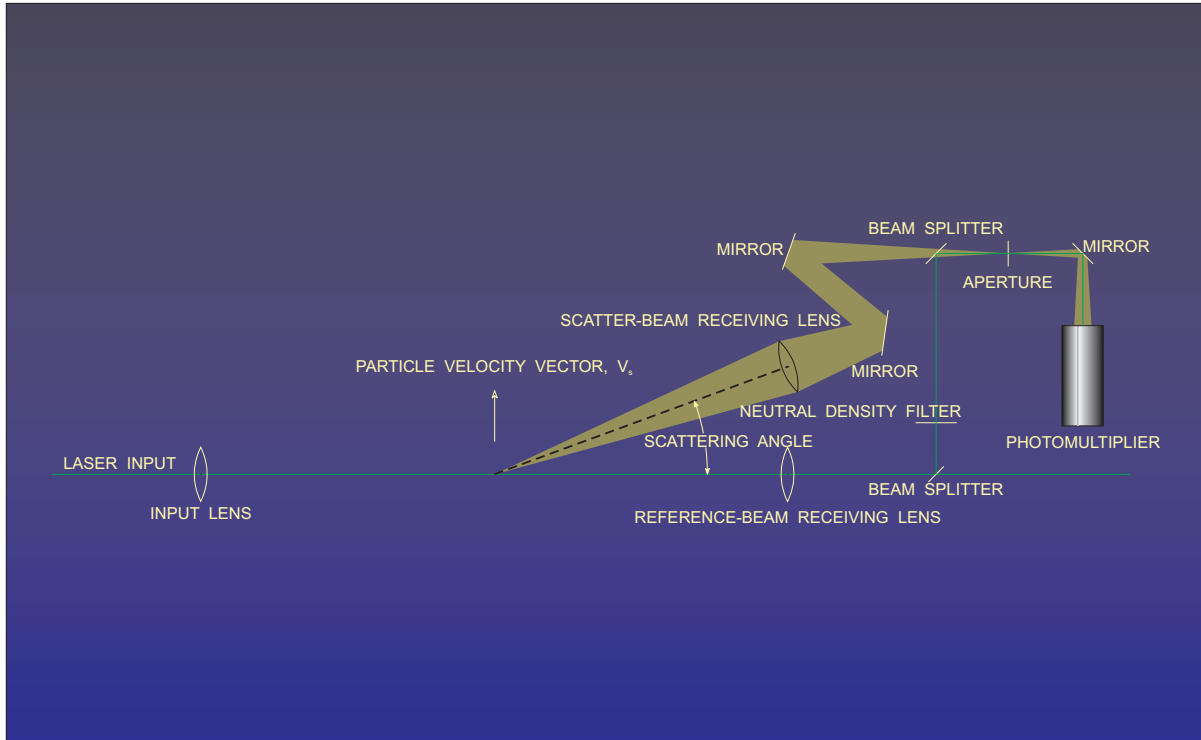


Figure 1.- Schematic of single-beam laser Doppler velocimeter.

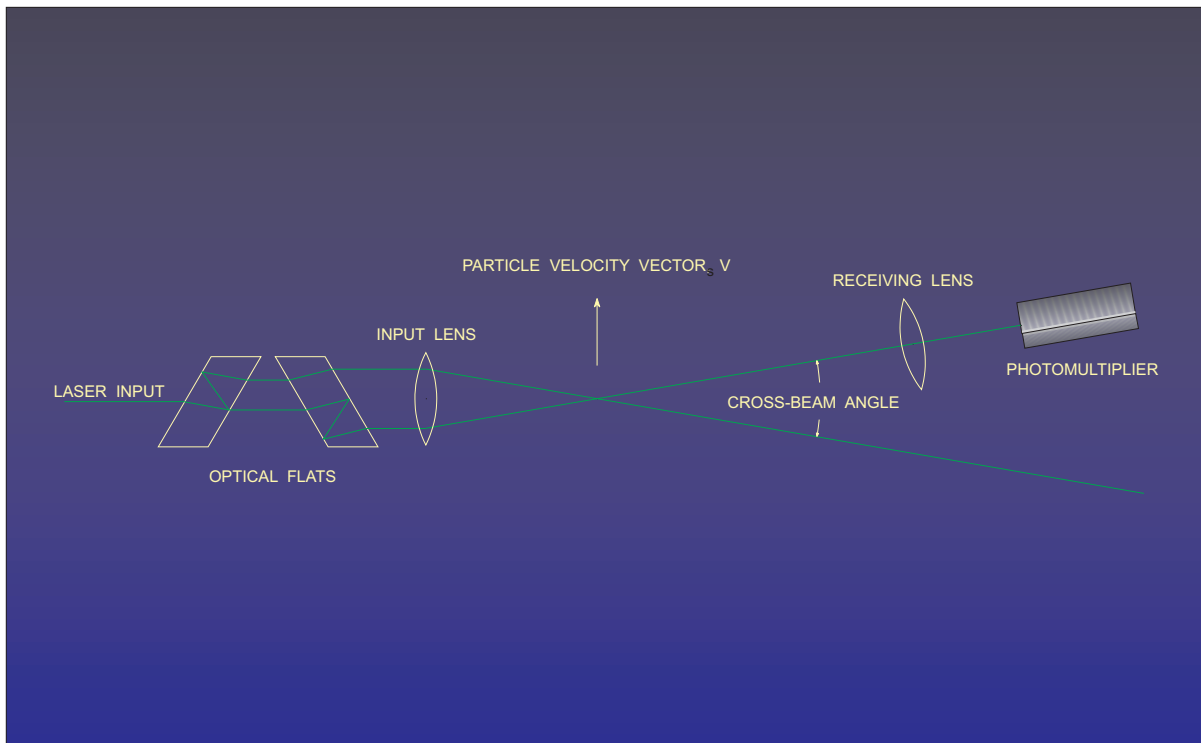


Figure 2.- Schematic of cross-beam laser Doppler velocimeter in reference-scatter mode.

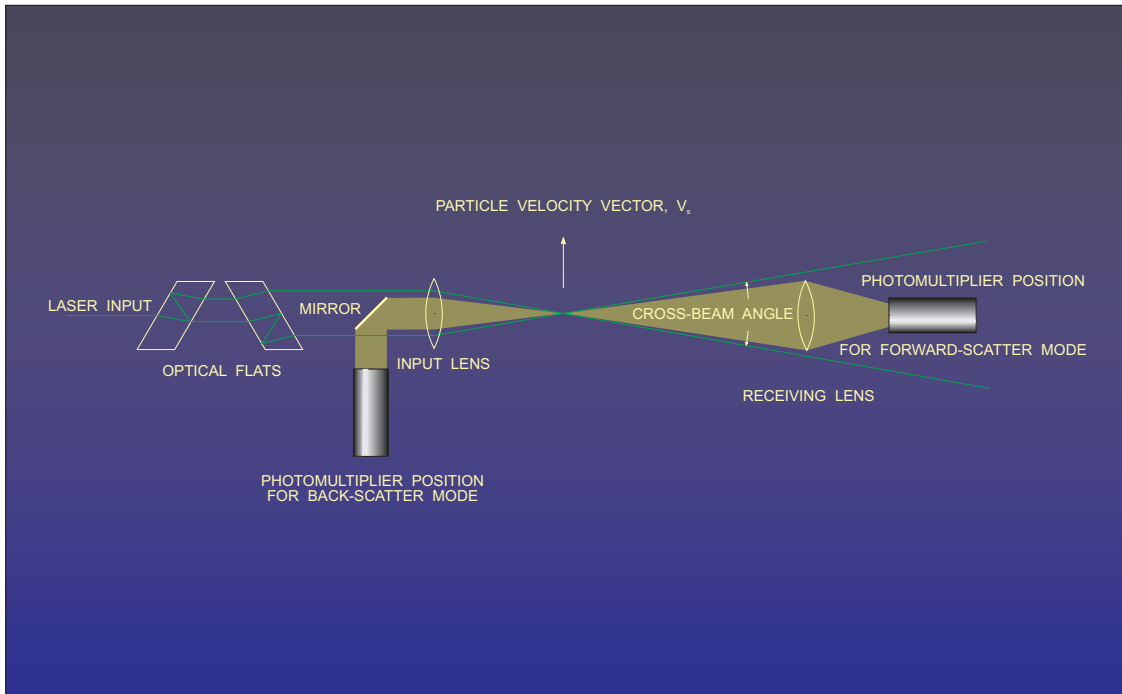


Figure 3.- Schematic of cross-beam laser Doppler velocimeter in dual-scatter-forward-scatter and dual-scatter-back-scatter modes.

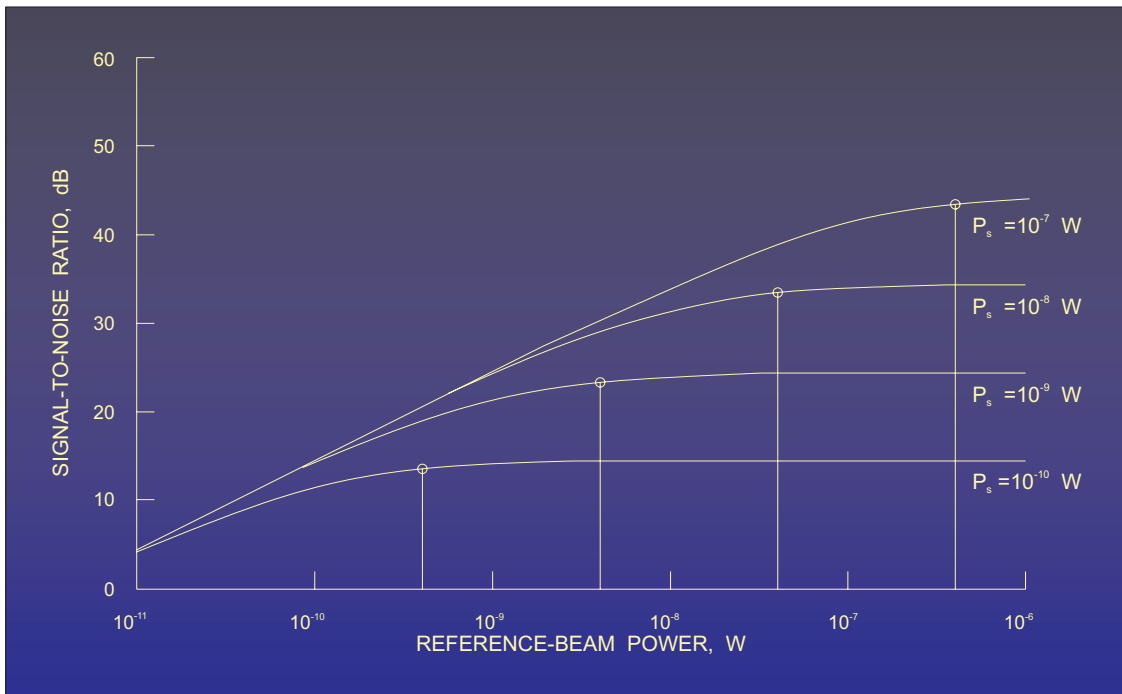


Figure 4.- Determination of minimum ratio of reference-beam power to scattered power P_r/P_s necessary for signal-to-noise ratio to be independent of reference-beam power. Plots of signal-to-noise ratio as a function of reference-beam power were determined for an Argon laser at 514.5 nm and a noise bandwidth of 10^6 Hz.

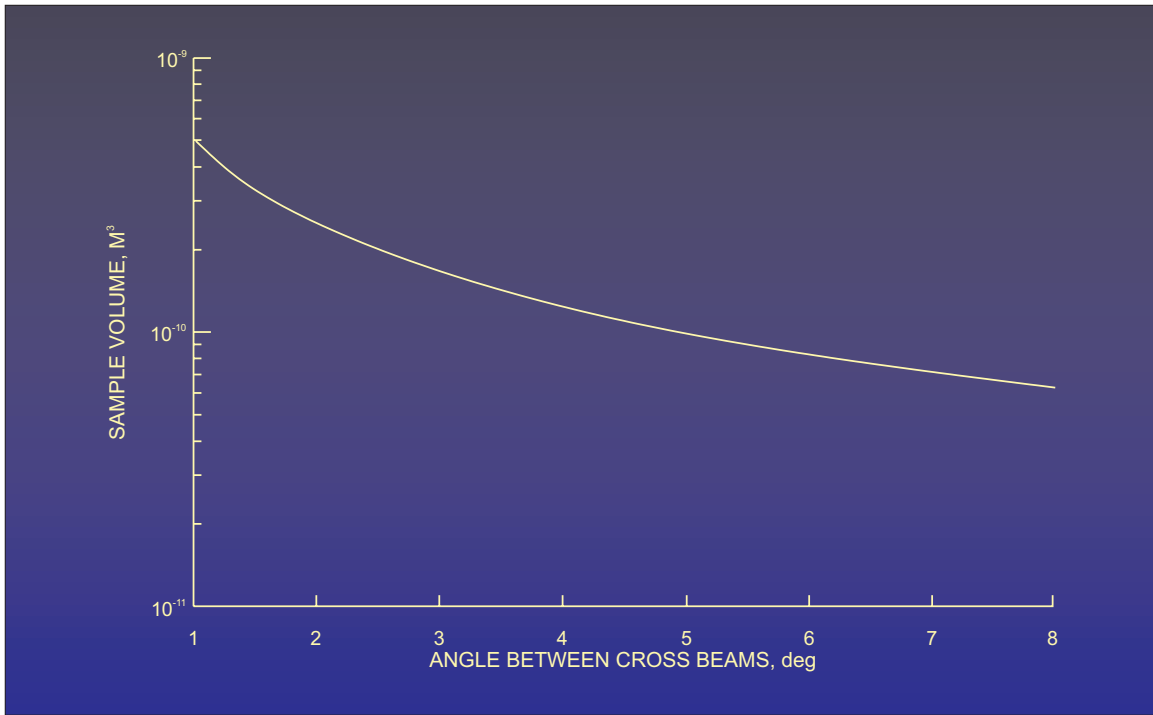


Figure 5.- Determination of sample volume viewed by input focusing lens, with local length 0.6096 m, of the LDV as a function of angle between the beams.

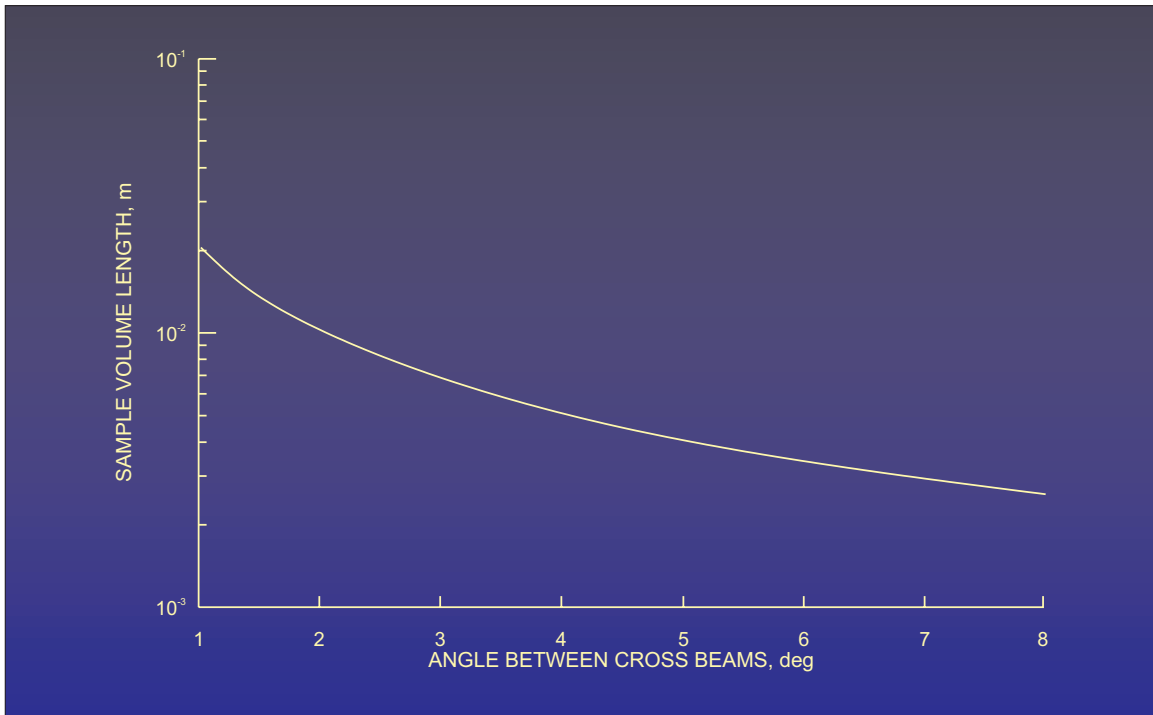


Figure 6.- Beam axis length of the sample volume as a function of cross-beam angle.

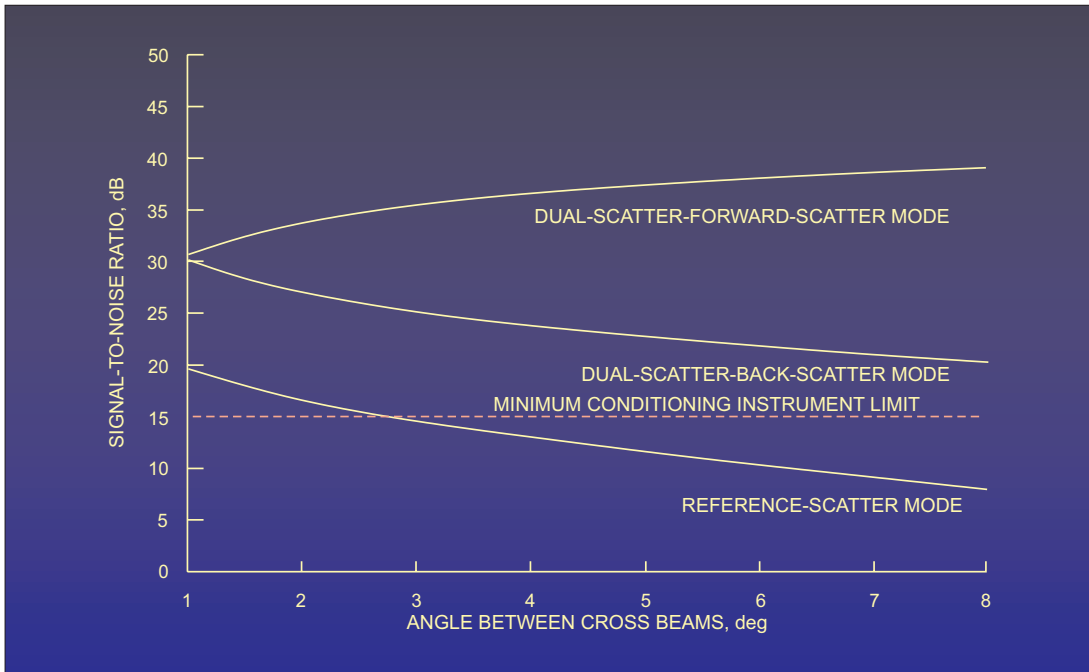


Figure 7.- Comparison of signal-to-noise ratio determined from a seeding density of 1000 particles/cm³ as a function of cross-beam angle for the three LDV modes using the 514.5 nm Argon laser line at 1.0 W and a noise bandwidth of 10⁶ Hz.

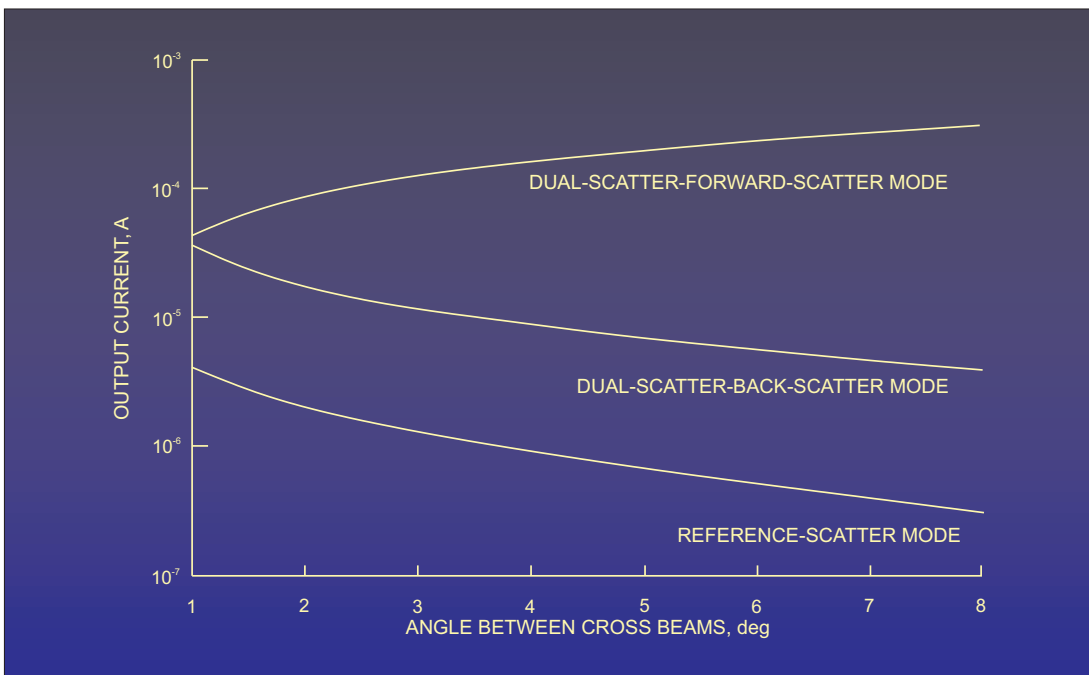


Figure 8.- Comparison of photomultiplier output current determined from a seeding density of 1000 particles/cm³ as a function of cross-beam angle for the three LDV modes using the 514.5 nm Argon laser line at 1.0 W.

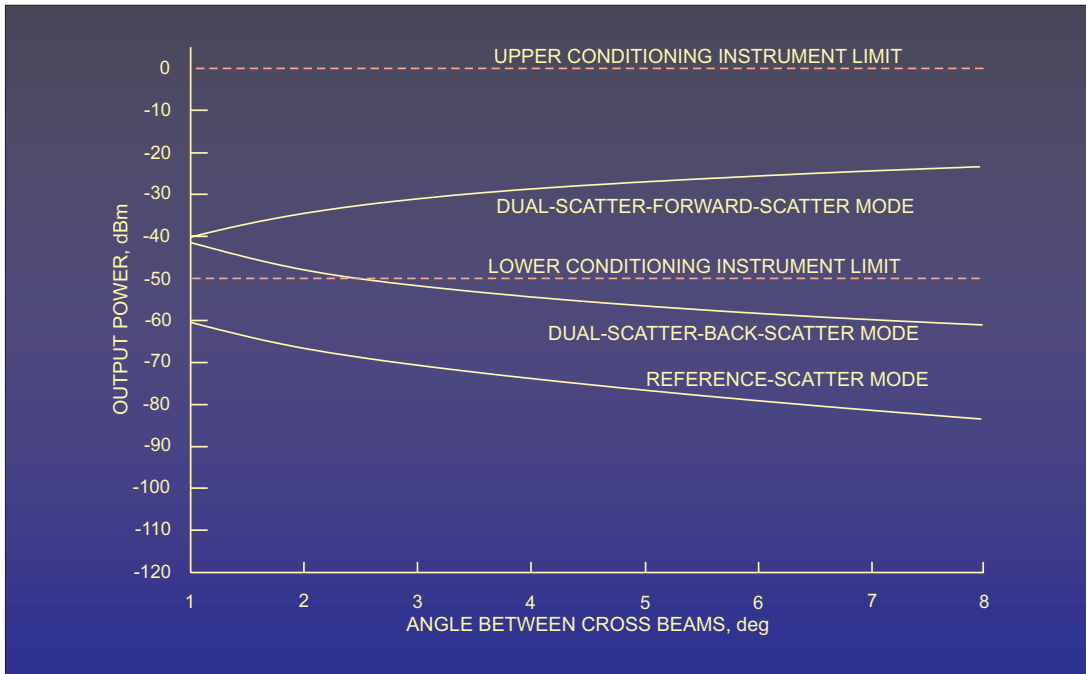


Figure 9.- Comparison of photomultiplier output power determined from a seeding density of 1000 particles/cm³ as a function of cross-beam angle for the three LDV modes using the 514.5 nm Argon laser line at 1.0 W.

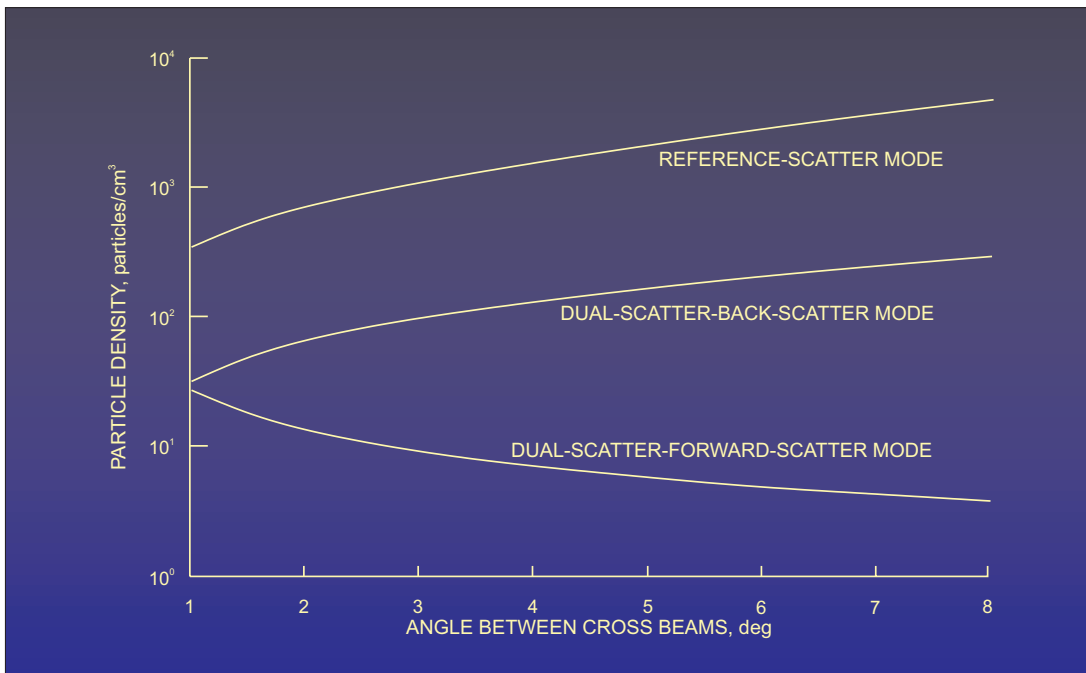


Figure 10.- Determination of required seeding density as a function of cross-beam angle for the three LDV modes using a signal-to-noise ratio of 15 dB, a noise bandwidth of 10⁶ Hz, and 514.5 nm Argon laser line at 1.0 W.

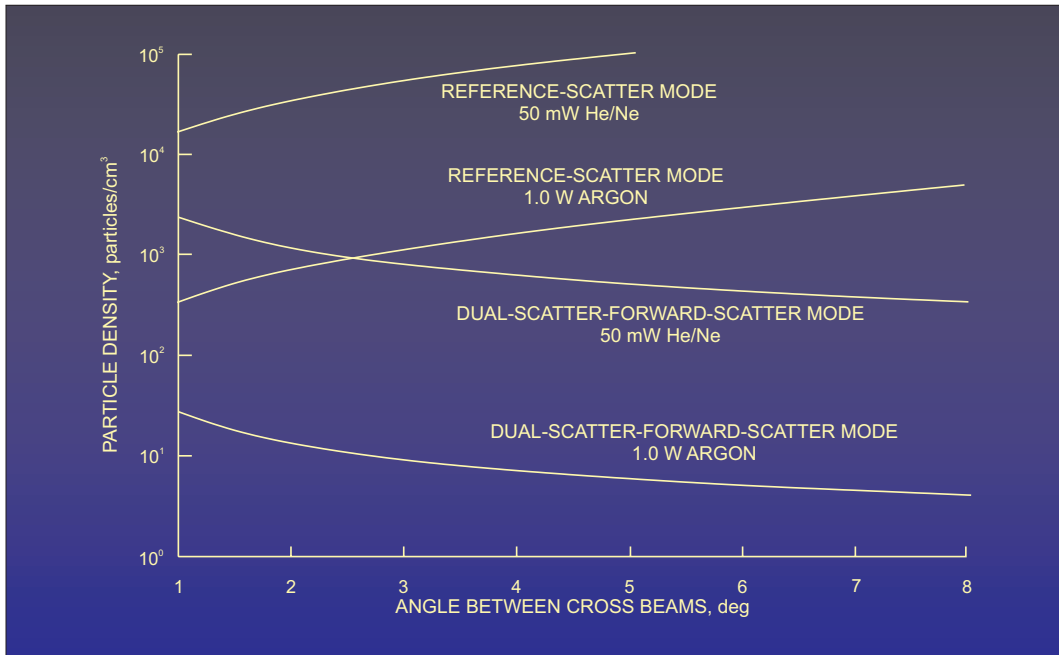


Figure 11.- Determination of required seeding density as a function of cross-beam angle for the dual-scatter-forward-scatter mode and the reference-scatter mode using a 50-mW He/Ne laser and a 1.0-W Argon laser at 514.5 nm for a signal-to-noise ratio of 15 dB and a noise bandwidth of 10⁶ Hz.

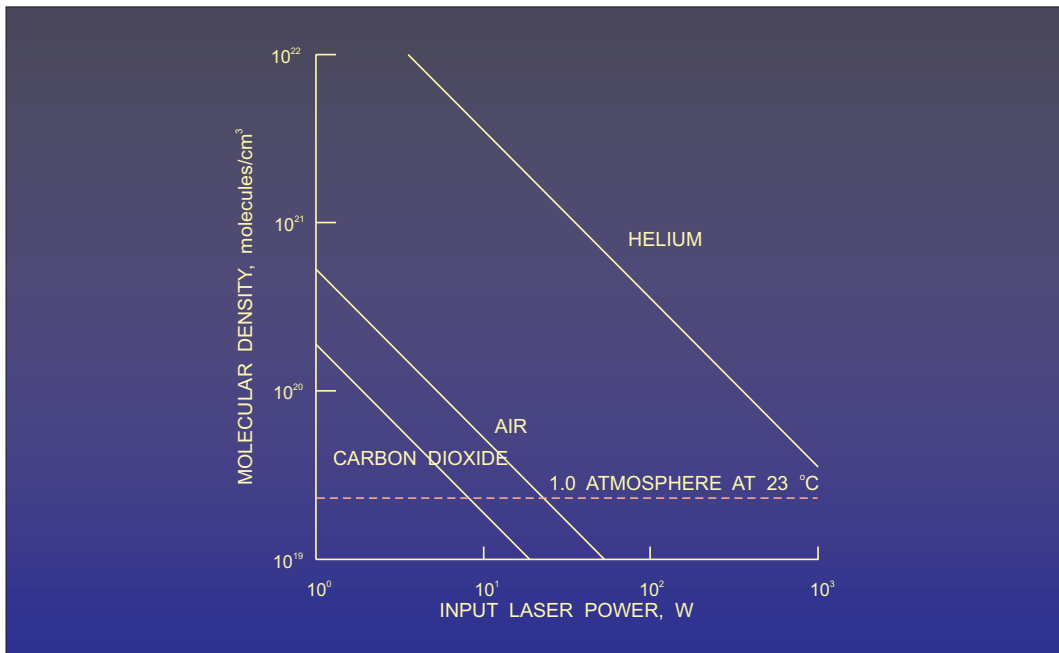


Figure 12.- Calculation of input laser power required to obtain molecular scatter needed for a signal-to-noise ratio of 15 dB using a 514.5 nm Argon laser line as a function of molecular density, with a noise bandwidth of 10⁶ Hz and an S-20 photomultiplier response.

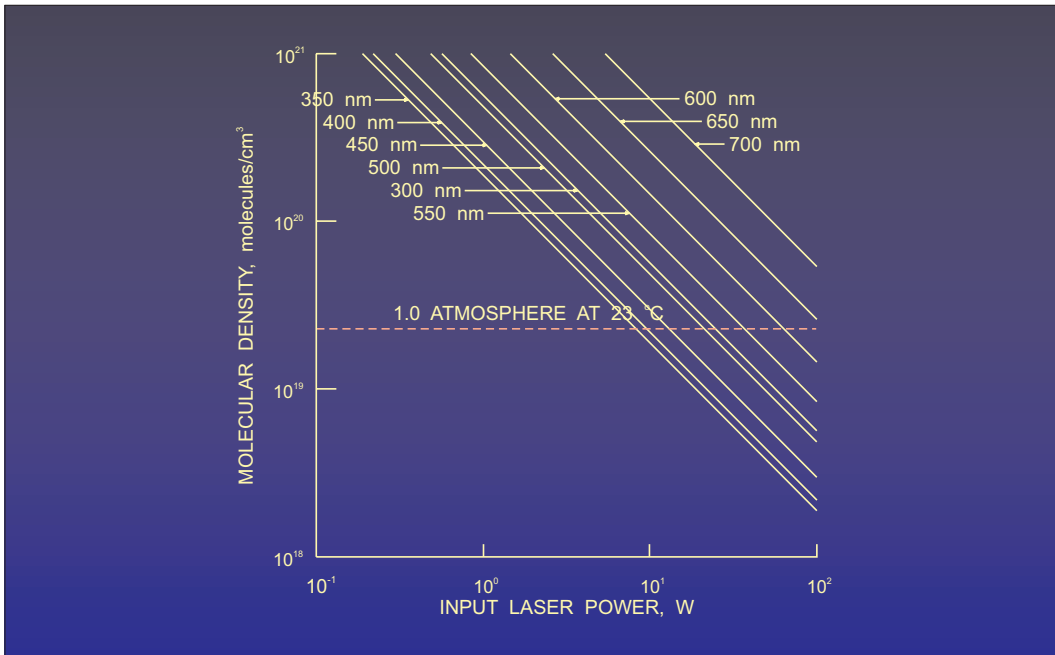


Figure 13.- Calculation of required input laser power to obtain molecular scatter needed for a signal-to-noise ratio of 15 dB as a function of molecular density for several light wavelengths in air, with a noise bandwidth of 10⁶ Hz and an S-20 photomultiplier response.

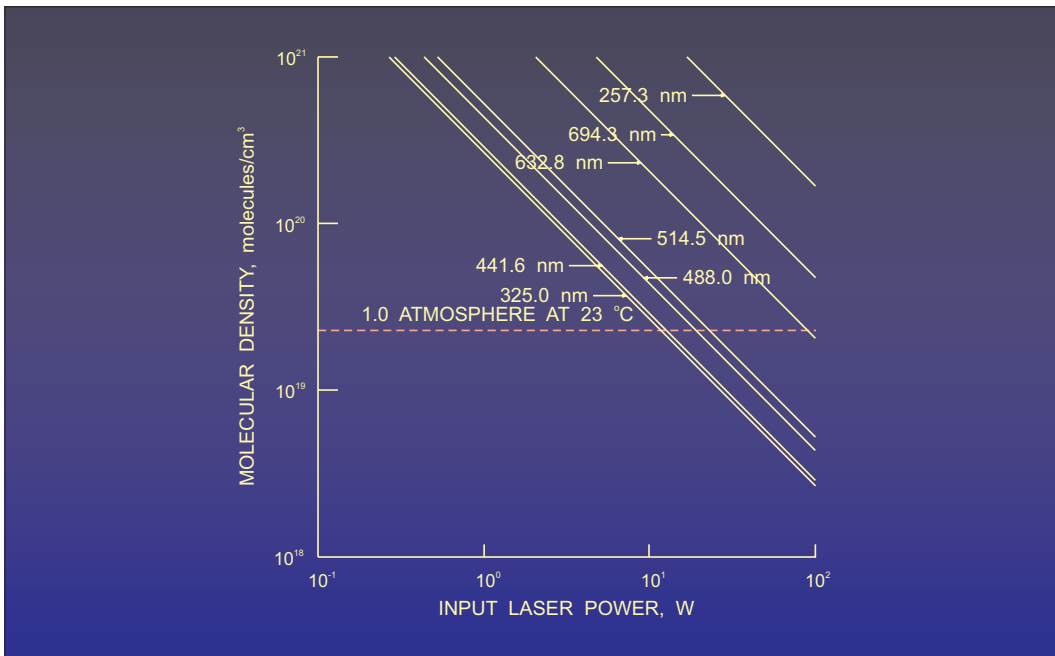


Figure 14.- Calculation of required input laser power to obtain molecular scatter needed for a signal-to-noise ratio of 15 dB as a function of molecular density for several laser wavelengths in air, with a noise bandwidth of 10⁶ Hz and an S-20 photomultiplier response.